INFORMATION TO USERS

This material was produced from a microfilm copy of the original document. While the most advanced technological means to photograph and reproduce this document have been used, the quality is heavily dependent upon the quality of the original submitted.

The following explanation of techniques is provided to help you understand markings or patterns which may appear on this reproduction.

1. The sign or "target" for pages apparently lacking from the document photographed is "Missing Page(s)". If it was possible to obtain the missing page(s) or section, they are spliced into the film along with adjacent pages. This may have necessitated cutting thru an image and duplicating adjacent pages to insure you complete continuity.

2. When an image on the film is obliterated with a large round black mark, it is an indication that the photographer suspected that the copy may have moved during exposure and thus cause a blurred image. You will find a good image of the page in the adjacent frame.

3. When a map, drawing or chart, etc., was part of the material being photographed the photographer followed a definite method in "sectioning" the material. It is customary to begin photoing at the upper left hand corner of a large sheet and to continue photoing from left to right in equal sections with a small overlap. If necessary, sectioning is continued again — beginning below the first row and continuing on until complete.

4. The majority of users indicate that the textual content is of greatest value, however, a somewhat higher quality reproduction could be made from "photographs" if essential to the understanding of the dissertation. Silver prints of "photographs" may be ordered at additional charge by writing the Order Department, giving the catalog number, title, author and specific pages you wish reproduced.

5. PLEASE NOTE: Some pages may have indistinct print. Filmed as received.

Xerox University Microfilms
300 North Zeeb Road
Ann Arbor, Michigan 48106

NUCLEAR MAGNETIC RESONANCE STUDIES ON PEPTIDE AGGREGATION: TYROCIDINE A--A MODEL SYSTEM

by

Martin Fein

A dissertation submitted to the Graduate Faculty in Biomedical Sciences, in Partial Fulfillment of the Requirements for the Degree of Doctor of Philosophy, The City University of New York

1975

This manuscript has been read and accepted for the Graduate Faculty in Biomedical Sciences in satisfaction of the dissertation requirement for the degree of Doctor of Philosophy.

9/8/75
date

Herman R. Wyssbrod
Chairman of Examining Committee

9/12/75
date

Terry Ann Knudsen
Executive Officer

W Scott
Joseph Fant
Patrick Aggena
Supervisory Committee

The City University of New York

Acknowledgements

I am grateful to the following people:

Dr. I. L. Schwartz for allowing me the freedom and flexibility that the pursuit of these studies required.

Dr. W. A. Gibbons for his generous supply of time and materials.

Drs. F. H. Field and W. C. Agosta for providing me with laboratory accommodations, access to the nmr facilities and, more importantly, continuing the atmosphere conducive to independent study set by the late Dr. L. C. Craig.

Peter Ziegler for providing assistance for me to run the instrument rather than for the instrument to run me.

Alan Fischman for providing the "friction"without which movement would not be possible.

Dr. D. A. Cowburn for not allowing my "scientific" reach to exceed its grasp--or perhaps it should be vice versa?

Dr. H. R. Wyssbrod for providing time for many useful discussions, effort into physical and mathematical analysis, the subtleties of which would have otherwise proved overwhelming, and for never letting the twelfth hour arrive.

Arlene--for just being.

TABLE OF CONTENTS

List of Tables

List of Figures

Page

CHAPTER I

INTRODUCTION

The non-covalent associations of proteins and peptides are a common denominator of all life. These molecules were, indeed, "designed" to have these properties. Natural selection is not very tolerant of any changes in primary structure which preclude these associations. She has, in fact, gone to great lengths to insure that these changes do not occur as evidenced by the degeneracy of the genetic code. Up to a point, this degeneracy enables changes in the genetic information to be compatible with life. For example, every amino acid containing U (uridylic acid residue) as the second "letter" of its codon is a hydrophobic amino acid (1). Thus, a change in the first and/or third "letter" would still lead to the incorporation of another hydrophobic amino acid. This mutation could be better tolerated than one in which a hydrophylic amino acid replaced the original amino acid.

The quaternary structure that these molecules attain is governed by the conformationally allowable formation of "weak" bonds (these bonds are discussed below). Like

tertiary structure, quaternary structure[1] is the attainment of the thermodynamically most stable state for this system. There is, however, usually more than one of these possible states whose energy is a minimum. Thus, given the tertiary structure of a peptide or protein that self-associates, there is no known "a priori" criterion by which one of several "most likely" structures is the predominating one. The complexity of this problem increases as the size and number of interacting subunits increases.

In an effort to characterize and gain insight into the physical and chemical requirements that govern conformation and subunit interactions in proteins, ample

---

1. The following definitions, based on concepts originally introduced by Linderstrøm-Lang (2), have been proposed by the IUPAC-IUB Commission on Biochemical Nomenclature (3):

   a. The primary structure of a peptide is the amino acid sequence of the peptide without regard to conformation (three-dimensional shape).

   b. The secondary structure of a peptide is the conformation of its main-chain atoms without regard to the conformation of its side chains--i.e., secondary structure and backbone conformation are identical terms.

   c. The tertiary structure of a peptide is the conformation of all of its atoms without regard to its relationship with neighboring molecular or subunits--i.e., tertiary structure is identical to backbone plus side-chain conformation.

   d. The quaternary structure is the arrangement of peptide subunits in space and the ensemble of its intersubunit contacts and interactions.

precedent has been set for the use of model systems. The characterization of the secondary and tertiary structure of a protein or peptide can be divided into a theoretical and an experimental attack.

The theoretical considerations take the form of energy calculations. In general, this approach attempts to limit the attainable conformations of the residues in a protein or peptide molecule by considering such factors as steric overlap, molecular orbitals, charges, etc., and minimizing the overall energy (4-7). Predictions based on this approach unfortunately usually result in more than one possible conformation.

The experimental approach to conformation and subunit interaction has at its disposal such techniques as x-ray diffraction, circular dichroism and optical rotatory dispersion, IR and UV spectrophotometry, and more recently, nmr spectroscopy and neutron diffrraction. To date, x-ray techniques provide the most precisely detailed picture of molecular conformation. This technique, however, is not suited to studying dynamic molecular processes. In addition, not every molecule can be suitably crystallized.

A good alternate technique to x-ray diffraction, and, at present, the most valuable form of nuclear magnetic resonance (nmr) spectroscopy for these studies, is proton magnetic resonance (pmr) spectroscopy. In theory, any

molecule that can be solubilized can be studied. From analysis of coupling constants, information can be obtained about conformation. Chemical shifts provide information about the electronic environment of individual nuclei--e.g., protons in the case of pmr studies. Solvent and temperature perturbations and exchange studies relate information about intramolecular hydrogen bonding. Spin-lattice relaxation time (T_1) measurements provide estimates of molecular size and motions.

As will be discussed, a reasonable model system to attempt a study of conformation and aggregation by nmr is provided by gramicidin S and the tyrocidines (Figure 1). These are all cyclic decapeptides. Gramicidin S and the tyrocidines are produced by different strains of Bacillus brevis at sporulation. The synthesis of these peptides are not directed by mRNA (8) but rather involve a thio-template mechanism (9) which some investigators believe is a primitive form of protein synthesis (10). Recent evidence suggests that the tyrocidines interfere with transcription and can bind to DNA (11, 12).

As a model system for studying aggregation it has previously been shown that gramicidin S does not self-associate to any appreciable extent, while the tyrocidines

Gramicidin S-A

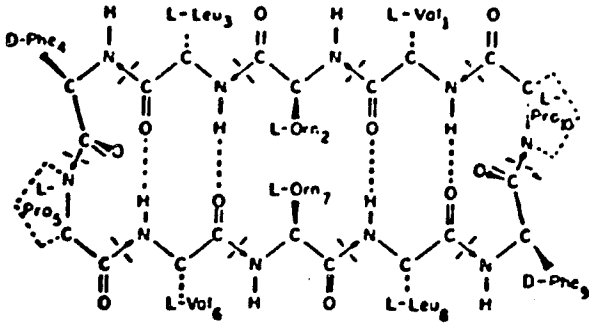

The Tyrocidines

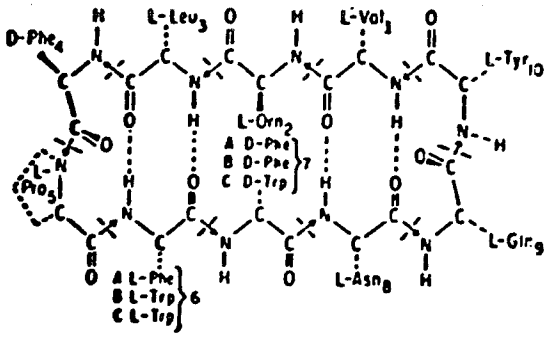

Tyrocidine A

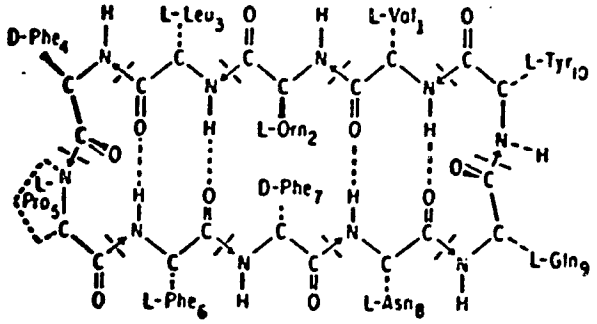

Figure 1

Secondary Structure (Backbone Conformation) of the Cyclic Decapeptide Antibiotics, Gramicidin S and the Tyrocidines.

The backbone atoms denoted by C and N lie approximately in the plane of the page. Flared and dashed bonds, respectively, adjoin groups in front of and back of this plane. Intramolecular hydrogen bonds are denoted by --- between H and O atoms.

under the same conditions exhibit extensive self-association (13-16). Ultracentrifugation and thin-film dialysis studies have shown that the tyrocidines aggregate in spite of such modifications as hydrogenation of their aromatic residues, iodination and methylation of the OH group of the tyrosyl residue and succinylation of the ϵ-NH_2 group of the ornithyl residue. Indeed, the only modification of the tyrocidines which prevented their aggregation was cleaving the backbone, which made them linear.

On the basis of these experiments it was concluded that the proper backbone conformation was a necessary requirement for aggregation. Just what forces--i.e., kinds of "weak" bonds--are involved in stabilizing the aggregate, however, remained elusive. The modifications of the ornithyl and tyrosyl residues preclude their participation in inter-molecular hydrogen bonds. Aromatic interactions could be ruled out on the basis of the results of the hydrogenation experiments and the additional observation that the tyrocidines differ among themselves only in their degree of aromaticity--i.e., substitution of tryptophyl for phenylalanyl residues--and still aggregate to the same extent. The only general class of "weak" bond that remains is the "hydrophobic bond."

Two factors are concerned with the formation and stabilization of "weak" bonds. Firstly, there is the tendency of groups to interact so as to minimize the overall energy, such as in the formation of a van der Waals bond, or to increase the overall entropy, such as in the formation of a "hydrophobic bond." Secondly, for there to be subunit-subunit interaction of any consequence, i.e., quaternary structure, the tertiary structures must create complementary surfaces so that the weakly interacting groups are properly juxtaposed.

The role of "weak" bonds is central to biological function. Current "dogma" states that the information necessary for the attainment of all higher-order (e.g., secondary and tertiary) structure is implicit in the primary sequence of a protein (17)--i.e., the linear sequence of a peptide or protein dictates the thermodynamically most stable state as expressed by the higher-order structures.

A "weak" bond is characterized by an energy of formation of between -0.5 and -10 kcal/mole. Large structures can be stabilized by the formation of a large number of such bonds. Thus, even though a particular "weak" bond can be broken by random thermal motion under normal environmental conditions, say at 20^{o}C, more of

them are maintained than disrupted on the average, thereby leading to a net stabilization effect on higher-order molecular structure. In general, all "weak" bonds are electrostatic in nature. As they occur in proteins, however, it is convenient to classify them as (1) salt bridges between charged groups such as $-NH_3^+$ and $-COO^-$, (2) hydrogen bonds, (3) van der Waals bonds, and (4) "hydrophobic bonds." Of all the "weak" bonds, the salt bridge is the one that is most electrostatic in nature. Van der Waals bonds result when the electrons in two neighboring groups repel one another, thereby creating two electrostatic dipoles that attract each other. The "hydrophobic bond," as defined by Kauzmann (18), is the proclivity of apolar groups to remove themselves from a polar environment. By doing so, the total entropy of the solute-solvent system increases by virtue of an increase in the number of configurational states the polar solvent molecules can attain--i.e., when apolar groups remove themselves, they release "ordered" bound solvent molecules, thereby increasing the total disorder (entropy) of the system.

In view of the homologies between gramicidin S and the tyrocidines, with respect to their primary structure, molecular size and weight, it is an intriguing

observation that such similar molecules should exhibit such antipodal behavior. Based on these considerations, it seems reasonable to hypothesize that the key to the aggregation behavior resides in the subtleties of molecular conformation which in the case of gramicidin S precludes the formation of these internuclear bonds while in the case of the tyrocidines allows them to be formed.

The secondary structure (backbone conformation) of gramicidin S in solution was deduced from nmr parameters (19). Previously, infrared dichroism experiments (20), x-ray data (21, 22) and energy minimization (23) had each yielded different conformational structures. The nmr approach to the conformation of gramicidin S yielded data which was consistent with one of the structures proposed x-ray studies. The nmr data to be rationalized consisted of vicinal amide-C^{α} proton coupling constants, hydrogen-deuterium exchange (HDX) and temperature perturbation of the amide proton chemical shifts, and explanation of anomalous chemical shifts.

Analysis of the coupling constants along with energy minimization considerations yielded the peptide backbone dihedral angles ϕ and ψ (ω is assumed to be 180^{o} in a

peptide bond).[2]

Temperature perturbations and HDX studies indicated that gramicidin S contained four solvent-shielded intramolecularly hydrogen-bonded amide protons and four solvent-exposed protons.

In addition, C_2 symmetry of the molecule was evidenced by only four separate proton signals for the eight amide protons and five signals for the ten C^{α} protons (i.e., each separate nmr signal corresponded to two protons in the molecule). In other words, the C^{α} protons in both ornithyl residues, for example, resonated at the same frequency, thereby indicating that these two protons experience, on the average, the same magnetic--and hence most probably the same chemical--environment.

The model for gramicidin S which is consistent with this data is an antiparallel β-pleated sheet containing two β-turns and four intramolecular, transannular hydrogen bonds (Figure 1).

---

2. Recent convention recommended by the IUPAC-IUB Commission on Biochemical Nomenclature is used to express dihedral angles (3). A value of 180° for ω corresponds to a trans configuration of the peptide linkage--i.e., to a trans arrangement of the amide H and carbonyl O atoms and to a trans arrangement of the two adjoining C^{α} atoms.

One would expect, in view of the homology between the first five residues of gramicidin S and those of the tyrocidines, that certain structural similarities should be present. Because of steric constraints, it is especially likely that such similarities should be manifest in the D-Phe^4-Pro^5 β-turn region (24, 25). Similarities in structure should, to some degree, be carried over into similarities in spectral parameters. In principle, this should aid in a conformational analysis of the tyrocidines. Lastly, the aggregation behavior of the tyrocidines could be contrasted with the non-aggregational behavior of gramicidin S in an nmr study. Hopefully, this comparison could enable one to make some suggestions regarding the quaternary structure of the aggregates.

CHAPTER II

CONFORMATION OF THE TYROCIDINES

A. Choice of a Solvent System

The force and utility of nmr studies of dynamic molecular processes such as aggregation reside in the ability of this method to display the entire molecule as it undergoes self-association. Thus, information about the backbone and side chains are simultaneously acquired. To achieve this end, the choice of a solvent is critical. Properties that render a solvent ideal for one technique, however, may be antithetical or unnecessary for another. This generates the problem of data correlation and interpretation for the same molecule studied in different solvents by different techniques.

The ultracentrifugation and thin-film dialysis studies on the tyrocidines, which provided estimates about aggregate size and weight, possible stoichiometries and thermodynamic parameters of aggregate formation, were performed in water and water/acetic acid mixtures (15). Fluorescence and phosphorescence studies, which provided evidence of a hydrophobic contribution to the self-association process, were performed in water and

methanol/water mixtures, respectively (26).

The nmr studies reported here were performed in fully deuterated dimethylsulfoxide ($(CD_3)_2SO$). The main objectives of these studies were the determination of molecular conformation(s) and quaternary structure(s). It is thus relevant to consider the contribution of a solvent to molecular conformation and whether correlations between studies in different solvents can be made.

The relative populations of rotomers and conformers[3] of a particular molecule change as a function of solvent polarity (27). The degree of change in secondary structure is, to a large extent, however, determined by the size and primary structure of the peptide. For random coil or large cyclic peptides, such as the cyclodepsipeptide valinomycin, solvent perturbations have profound conformational effects. Ivanov et al. have found that, in going from CCl_4 to $(CD_3)_2SO$, the conformational states

---

3. Some peptides are thought to possess more than one relatively stable conformation in solution. These different conformations, which are generally in a state of equilibrium with one another, are called conformers. In this dissertation conformers refers to the different conformational forms of the backbone (secondary structure). Even peptides that are thought to possess only one stable backbone conformation may manifest extensive conformational averaging in their side chains. In this dissertation different side-chain conformational forms are called rotomers. Thus, gramicidin S is thought to consist essentially of a single conformer, but that conformer consists of many different rotomers.

of valinomycin are altered (28). The predominant conformation of valinomycin in CCl_4, with a dielectric constant ϵ of 2.2, has all six amide protons involved in the formation of intramolecular hydrogen bonds. When valinomycin was studied in $(CD_3)_2SO$, with a dielectric constant of 46.6, it was found that three of the amide protons became hydrogen bonded to the solvent. The complexities of this molecule include a 36-membered backbone containing both amide and ester linkages.

Solvent-dependent conformational changes are somewhat winnowed when cyclic peptides, both model and naturally occurring, whose backbones contain from 6 to 10 amide linkages are considered. The interaction can be simplified further if amino acid residues that restrict the number of attainable conformations (e.g., the prolyl residue) are incorporated into the backbone or if some other conformational restraint such as metal complexation is present.

Llinás et al. (29-31) studied the cyclohexapeptide ferrichrome. The studies were conducted in both D_2O and $(CD_3)_2SO$ on the aluminum-substituted chelate and the free, uncomplexed deferri structure. The nmr parameters of the chelate indicated that the backbone conformation was solvent-independent. In addition, comparison of the data for the free and complexed molecule in $(CD_3)_2SO$ also

indicate the same conformation. In contrast to these findings, the deferri structure differs from the chelate in water. This indicates that there is some conformational change in the uncomplexed molecule as a function of solvent polarity. Perhaps, not surprisingly, the main differences concerned those residues which were involved in complexing the metal. Finally, information about intramolecular hydrogen bonding in the uncomplexed molecule in water could not be obtained because of exchange broadening. Therefore, the constraint imposed by chelation removed some of the flexibility and thus limited the most stable conformation.

Inclusion of a prolyl residue in the primary structure of peptides provides another mechanism of conformational constraint. The presence of a prolyl residue covalently bonded to a D-amino acid provides favorable conditions for formation of a β-turn arrangement (24, 25). β-Turns involve four consecutive amino acid residues with the inner two residues in a rather restrictive secondary structure. A single β-turn in a cyclic decapeptide accounts for 20 percent of the secondary structure. In the case of gramicidin S, which contains two β-turns, 40 percent of the backbone conformation is concerned with the formation of these structures (19).

Hence, the amount of conformational change that can be induced by solvents of differing polarities in small cyclic peptides containing β-turns would not be expected to cause gross changes in secondary structure. Changes that may be expected are number and strength of intramolecular hydrogen bonds, depending on their solvent accessibility, and changes in side-chain rotomer populations. Solvent perturbation studies on tyrocidine A, to be reported below, are consistent with the above generalizations.

The solvent characteristics required for nmr investigations of conformation and aggregation are as follows:

(i) The peptide must be soluble over a range sufficient to observe aggregation.

(ii) The solvent spectrum should not obscure any region of the peptide spectrum.

(iii) The solvent should not promote the exchange of labile protons (e.g., amide protons), thus allowing for visualization of the entire molecule.

(iv) The solvent should be chemically inert.

(v) The solvent should be stable over a moderate range of temperatures.

All these criteria are met in the study of gramicidin S and the tyrocidines in $(CD_3)_2SO$. In addition, the

dielectric constant of $(CD_3)_2SO$ allows it to form hydrogen bonds with solvent-exposed amide protons.

The use of water as a solvent in these nmr studies is actually contraindicated. Aggregation of the tyrocidines has been induced by increasing the proportion of water in a water-$(CD_3)_2SO$ mixture, while maintaining the peptide concentration constant. One must then, however, resolve spectral differences due to aggregation from those produced by changes in solvent polarity per se.

Since the tyrocidines are only sparingly soluble in water, only very low concentrations can be studied. Studies at low concentration can be performed most efficiently by using a special technique such as the pulse and Fourier transform nmr (ftnmr) method. To obtain acceptable signal-to-noise levels, it would be necessary to collect repeated scans of a particular spectrum. For low concentrations of tyrocidine in water, it may be necessary to collect thousands of scans. Thus, a prohibitive amount of time would be required to collect even a small amount of data. Furthermore, since the water protons are the predominant species in the sample, their signals will monopolize the dynamic range of the data acquisition system, thereby leading to a loss in the

ability to digitize with sufficient precision the signals from the protons in the peptide. In addition, the dynamic range problem is compounded by the fact that the chemical shift of the water protons overlaps portions of the C^{α} proton region and thus obscures it.

Substitution of D_2O for H_2O would alleviate the problems mentioned above, but would lead to the exchange of the labile amide protons. This exchange results in a loss of valuable information about secondary structure.

Aggregates of the tyrocidines attained in water can reach formidable sizes, about 32,400 daltons (15). Thus, nmr studies of these aggregates would be tantamount to those of a protein, and information normally inherent in high-resolution spectra of small molecules would not be obtained from the relatively low-resolution spectra of the large aggregates.

Lastly, as a function of temperature, the amide proton signals would be broadened in water by exchange, This broadening would interfere with the determination of coupling constants, chemical shifts and analysis of hydrogen bonding.

One of the most important considerations in studying aggregation is that of peptide solubility. If the rate of formation and resulting size of the aggregate is too

great, then only the end points of the process can be studied. The intermediate stages would never be "seen." On the basis of this consideration, $(CD_3)_2SO$ is a good solvent. Furthermore, relatively high peptide concentrations ranging from 1 mg/ml to greater than 250 mg/ml can be studied.

The detrimental aspects of $(CD_3)_2SO$ as a solvent include possible alterations in the extent of cooperative interactions--i.e., micelle formation and critical micelle concentration--due to its decreased polarity relative to water. Attempts to obtain estimates of molecular weights in $(CD_3)_2SO$ by vapor-pressure osmometry were unsuccessful because of the low vapor pressure of this solvent.

B. Spectral Assignments of Tyrocidine A

The spectral assignments of tyrocidine A were based on the following studies and comparisons:

(i) Decoupling experiments.

(ii) Temperature perturbations of the chemical shifts of the amide protons.

(iii) A solvent perturbation of the chemical shifts of the amide protons.

(iv) Hydrogen-deuterium exchange (HDX) experiments.

(v) Analysis of vicinal amide-C^{α} proton coupling constants.

(vi) Analogy with spectral parameters of gramicidin S.

(vii) Analysis of a Corey-Pauling-Koltun (CPK) molecular model.

1. Decoupling Experiments

Materials and Methods: Tyrocidine A was purified from a mixture of the tyrocidines via counter-current distribution (32, 33). The sample was prepared by dissolving 40 mg of purified tyrocidine A in 0.8 ml $(CD_3)_2SO$ (99.9 percent D).

The proton magnetic resonance (pmr) spectra were obtained on the consortium-operated Varian HR-220 field-sweep spectrometer located at the Rockefeller University. This instrument was operated in the continuous wave (CW) mode. Spin decoupling was performed using the field-track technique.

Results and Discussion: The side-chain (e.g., β-, γ-, and δ-protons) were assigned on the basis of their chemical shifts--i.e., by comparison of the spectrum of the peptide to the spectra of the individual free and methyl N-acetyl derivatives of the amino acids. Resonances

of side-chain protons are usually relatively invariant with reference to their chemical shifts and multiplicities and as such serve as convenient landmarks in making assignments.

C^{α} protons were assigned by decoupling them from their respective vicinal C^{β} protons by double-resonance experiments. (The C^{α} proton of the prolyl residue was assigned by other criteria described below.) Amide protons were then assigned by double-resonance experiments in which they were decoupled from their respective vicinal C^{α} protons.

The assignment of the prolyl C^{α} proton at 4.09 ppm (900 Hz) was based on negative evidence provided by the following observations:

(i) The multiplicity of the resonance remained unchanged after all the amide protons had been exchanged for deuterium (the prolyl residue does not possess an amide proton).

(ii) Double-resonance experiments failed to show any coupling between this C^{α} proton signal and any amide proton signal.

(iii) No coupling between this C^{α} proton signal and any C^{β} proton signal assigned to other residues could be detected by double-resonance experiments.

There were three regions of spectral overlap which introduced ambiguities into assignments based on the double-resonance experiments. The C^{β} proton resonances of the four aromatic residues (D-Phe^4, L-Phe^6, D-Phe^7 and Tyr^{10}) are contained in an envelope in the region of 2.73-3.09 ppm (660-680 Hz). Therefore, they could not be assigned to specific aromatic C^{α} protons by decoupling. This ambiguity, therefore, was also propagated into the assignments of specific aromatic amide protons by the double-resonance technique.

There was spectral overlap of the resonances of the two C^{α} protons located at 4.32 ppm (950 Hz). Double-resonance experiments unequivocally show them to belong to aromatic residues (D-Phe^4 and L-Phe^6), but due to the overlap of the resonances of the C^{β} protons of the aromatic residues, as discussed above, specific assignments could not be made by this technique.

The envelope of the resonances of four C^{α} protons centered at 4.56 ppm (1000 Hz) were partially resolved by decoupling into two sets, one corresponding to further unresolvable resonances of the C^{α} protons of Val^1 and Leu^3 and the other corresponding to those of Asn^8 and Tyr^{10} (34).

Complete and unequivocal assignments of the proton resonances of the four aromatic residues, as well as the amide protons of Val^1 and Leu^3, require obtaining spectra of tyrocidine A analogues with selectively deuterated amino acid residues. Unfortunately, the synthesis of the tyrocidines was not available at the time the decoupling experiments were performed.[4]

The decoupling experiments can, however, be augmented by information obtained from the homology between residues 1-5 of gramicidin S and the same residues of tyrocidine A, solvent and temperature perturbations of the amide protons and analysis of the observed vicinal amide-C^{α} proton coupling constants (J) by the appropriate Karplus relationship (35, 36) that relates ϕ and J (37, 38).

2. Studies of Hydrogen Bonding of Backbone Amide Protons

Methods for studying hydrogen bonding by nmr include hydrogen-deuterium exchange (HDX), temperature dependence of the chemical shifts, solvent perturbations (39) of the chemical shifts and the line-broadening agents such as free radicals or relaxation reagents (40). The

---

4. A workable synthesis of the tyrocidines was achieved in our laboratory in June, 1975.

rationale behind all these methods is that intramolecularly hydrogen-bonded protons are less available for interaction with the solvent or reagent and are thus less likely to be affected by them. This concept must be interpreted carefully when using line-broadening reagents. The magnitude of the perturbation depends upon the distance of the perturbed proton from the reagent and upon their relative orientation.

In a peptide, the reagent may have an affinity for a particular side chain. Complexation of this locus would cause disturbances throughout a region of space. Any proton within this region would be affected, regardless of its hydrogen-bonded state.

The basis of an HDX experiment relies on the inability of the spectrometer to detect the deuterium resonances when the instrument is set for protons. As the labile amide protons (hydrogen atoms) exchange for deuterium atoms (either from solvents such as CD_3OD or from added D_2O) the signal intensity decreases and ultimately disappears. This exchange is a pseudo-first order reaction which obeys the following equation:

$$I = I_0 e^{-kt}$$

where I_0 is the maximum intensity, I is the intensity at any time t after the addition of exchangeable deuterium,

and k is the rate constant. Taking natural logarithms of the above equation yields the following linear equation:

$$\ln I = \ln I_0 - kt$$

Plotting ln I as a function of t should yield a straight line with intercept ln I_0 and slope -k. The slope--and hence the rate constant k--may be obtained either graphically or by calculation with a linear regression program.

The rate of exchange for a given proton is subject to certain experimental conditions. The rate will vary as a function of pH, temperature and mole fraction of added solvent-containing exchangeable dueterium--e.g., D_2O. For a fixed set of conditions, the exchange rate of a particular amide proton is then a reflection of the solvent accessibility of that proton.

Rapidly exchanging protons are unequivocally solvent-exposed. Amide protons that exhibit slow exchange do so in general because of inaccessibility to solvent. Inaccessibility may be caused by involvement in an intramolecular hydrogen bond or due to steric factors which shield a proton from solvent interactions. Hence, in the case of a proton with a slow exchange rate, additional information is necessary to determine if it is indeed intramolecularly hydrogen-bonded.

Temperature perturbations of amide proton chemical shifts provide a complementary method to HDX studies for detecting intramolecular hydrogen bonding. In general, the formation of a hydrogen bond results in a decreased electron density around the participating proton. This deshielding of the proton is reflected in the increased energy necessary to achieve resonance. Consequently, a hydrogen-bonded proton absorbs in the downfield region of the spectrum (41).

While this behavior is generally true of hydrogen-bonded protons in organic compounds it must be modified for cyclic peptides. In these molecules, studied in $(CD_3)_2SO$), the signals of amide protons involved in transannular intramolecular hydrogen bonds occur upfield from those of solvent-exposed amide protons (15, 29). There are two contributions which can lead to this apparently anomalous behavior. In solvents of high dielectric constant such as water and $(CD_3)_2SO$, a proton involved in a hydrogen bond with the solvent may be relatively more deshielded than a proton hydrogen bonded to a carbonyl group. Secondly, a transannularly hydrogen-bonded amide proton is subject to anisotropic diamagnetic shielding from contiguous carbonyl π bonds (15, 42).

Thus, the observed chemical shift is a result of the net shielding or deshielding experienced by the proton.

Regardless of its chemical shift, a proton involved in a hydrogen bond with the solvent is subject to perturbation by thermal processes. As the temperature is increased, a greater proportion of these bonds are, on the average, broken than maintained. As a result of this, the proton becomes increasingly more shielded with increasing temperature and thus resonates at higher and higher magnetic field strengths. Upfield shifts with increasing temperature therefore are characteristic of solvent-exposed protons.

In contrast to this behavior, an intramolecularly hydrogen-bonded proton is subjected to virtually the same environment throughout the temperature range of the experiment. Consequently, its electron density, and hence its effective magnetic field, are unaltered. This means that its resonance energy does not change; therefore, its chemical shift does not change. An intramolecularly hydrogen-bonded amide proton is characterized by a low temperature dependence of its chemical shift.

Interpretation of temperature studies are subject to the same restrictions as are HDX experiments. Both techniques are limited to probing proton-solvent

interactions. Either technique alone may not provide proof for the existence of an intramolecular hydrogen bond. Together, however, they provide criteria for determining the probable occurrence of such a bond. This approach is further strengthened by combination with studies of model compounds in solvents with known properties (43).

The picture that emerges for transannularly hydrogen-bonded amide protons in cyclic peptides studied in $(CD_3)_2SO$ is that they can be characterized by:

(i) Relatively upfield chemical shifts.

(ii) Very low temperature coefficients of their chemical shifts.

(iii) Slow HDX rates--i.e., small rate constants.

All other things being equal, the stronger the hydrogen bond, the lower the temperature dependence of the chemical shift and the slower the exchange rate. Hydrogen bonds, however, can exist in a range of distances between H and O atoms and of angles between the NH and CO bonds--i.e., in a range of strengths. Consequently, hydrogen-bonded H atoms manifest a range of chemical shifts and exchange rates.

a. Temperature Dependence of the Chemical Shifts of the Amide Protons

Materials and Methods: Purified tyrocidine A was dissolved in $(CD_3)_2SO$ or CH_3OH, 25 mg/0.7 ml, with tetramethylsilane (TMS) as an internal reference. Spectra were obtained of the amide-aromatic proton region by operating the spectrometer in the CW mode. Temperature calibration was performed by measuring the chemical shift difference between the methylene and hydroxyl protons of ethylene glycol at each temperature (this difference as a function of temperature is known). The accuracy of the system for this measurement was $\pm$ 2°C. The sample was then placed in the probe and allowed to come to thermal equilibrium with its surroundings. The state of equilibrium was ascertained by the absence of any further changes in chemical shifts as a function of time at each temperature. The spectra were recorded at a sweep width of 500 Hz and a sweep time of 500 seconds--i.e., the spectra were swept at 1 Hz/sec. In the analyses of the spectra, the chemical shifts of amide protons whose resonances were not overlapping were determined to within $\pm$ 1 Hz, while the uncertainty was estimated to be $\pm$ 2 Hz for those whose resonances did overlap.

Results and Discussion: The data are presented in Figures 2 and 3 and summarized in Table I.

On the basis of its temperature dependence, each amide proton can be placed empirically into one of three classes. Those protons with dependences from 0 to -3.0 ppb/^{o}C, low temperature dependence; those with dependence between -4.0 and -8.0 ppb/^{o}C, high temperature dependence; and those protons with dependences between -3.0 and -4.0 ppb/^{o}C, borderline temperature dependence.

A low temperature dependence is equated with participation in an intramolecular hydrogen bond (42, 44). The data for tyrocidine A in $(CD_3)_2SO$ suggest that Leu^3 and Asn^8 are unequivocally intramolecularly hydrogen-bonded and that those of Orn^2, D-Phe^4 and D-Phe^7 are solvent-exposed--hence, not intramolecularly hydrogen-bonded--as indicated by their large temperature dependences. The amide protons of L-Phe^6, Gln^9 and Tyr^{10} fall into the borderline class of temperature dependences. These may be involved in an intramolecular hydrogen bond or sterically shielded from interaction with solvent due to the conformation of the molecule.

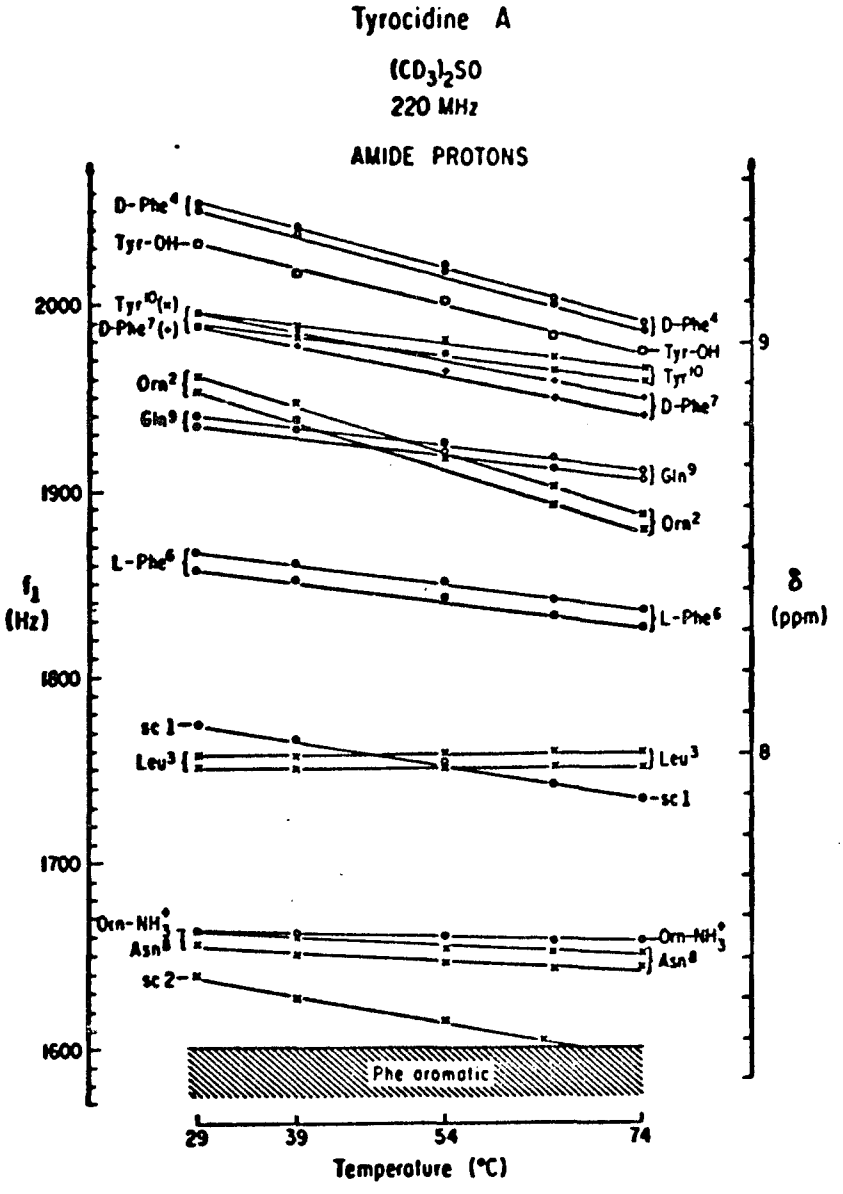

Figure 2

Temperature Dependence of the Chemical Shifts of the Amide Protons of Tyrocidine A in $(CD_3)_2SO$

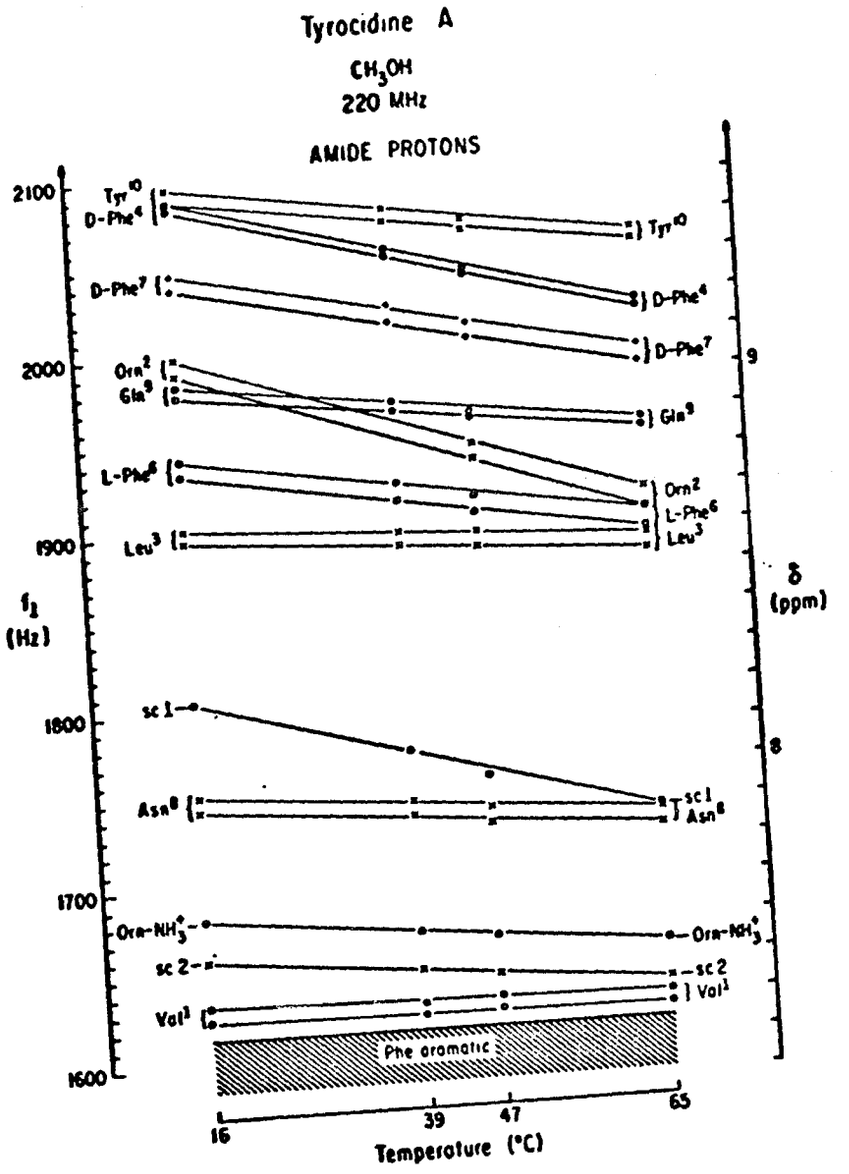

Figure 3

Temperature Dependence of the Chemical Shifts of the Amide Protons of Tyrocidine A in CH_3OH

Table I

Temperature Dependence of the Chemical Shifts of the Backbone Amide Protons of Tyrocidine A

Residue	$(CD_3)_2SO$	CH_3OH
	$\Delta\delta_{NH}/\Delta T$ (ppb/°C)	
L-Val[1]	Obscured	0.0
L-Orn[2]	-7.4	-8.0
L-Leu[3]	0.0	-1.4
D-Phe[4]	-6.5	-6.3
L-Pro[5]	-	-
L-Phe[6]	-3.1	-3.7
D-Phe[7]	-4.6	-4.9
L-Asn[8]	-1.2	-1.7
L-Gln[9]	-3.1	-2.9
L-Tyr[10]	-3.0	-3.2

The temperature-dependence data from the experiments in which methanol (CH_3OH) was the solvent are in good agreement with those in which $(CD_3)_2SO$ was the solvent and, in addition, provide information for the Val^1 amide proton whose resonances are no longer obscured by those of the aromatic protons in CH_3OH. The low temperature-dependent class amide protons consist of those of those of Val^1, Leu^3, Asn^8 and Gln^9. The high temperature-dependent class of backbone amide protons consists of those of Orn^2, D-Phe^4, D-Phe^7, while the amide protons of L-Phe^6 and Tyr^{10} comprise the borderline class of temperature-dependent chemical shifts.

The correlation between the temperature-dependence data in $(CD_3)_2SO$ and that in CH_3OH are presented in Figure 4. In both solvents the data are consistent with the existence of three classes of temperature-dependent behavior.

Based on the behavior in both solvents, it can be concluded that the amide protons of Val^1, Leu^3 and Asn^8 are involved in the formation of transannular hydrogen bonds. The amide protons of Orn^2, D-Phe^4, and D-Phe^7 are clearly solvent exposed--i.e., not intramolecularly hydrogen-bonded. The temperature-dependence studies do not provide unequivocal evidence of intramolecular

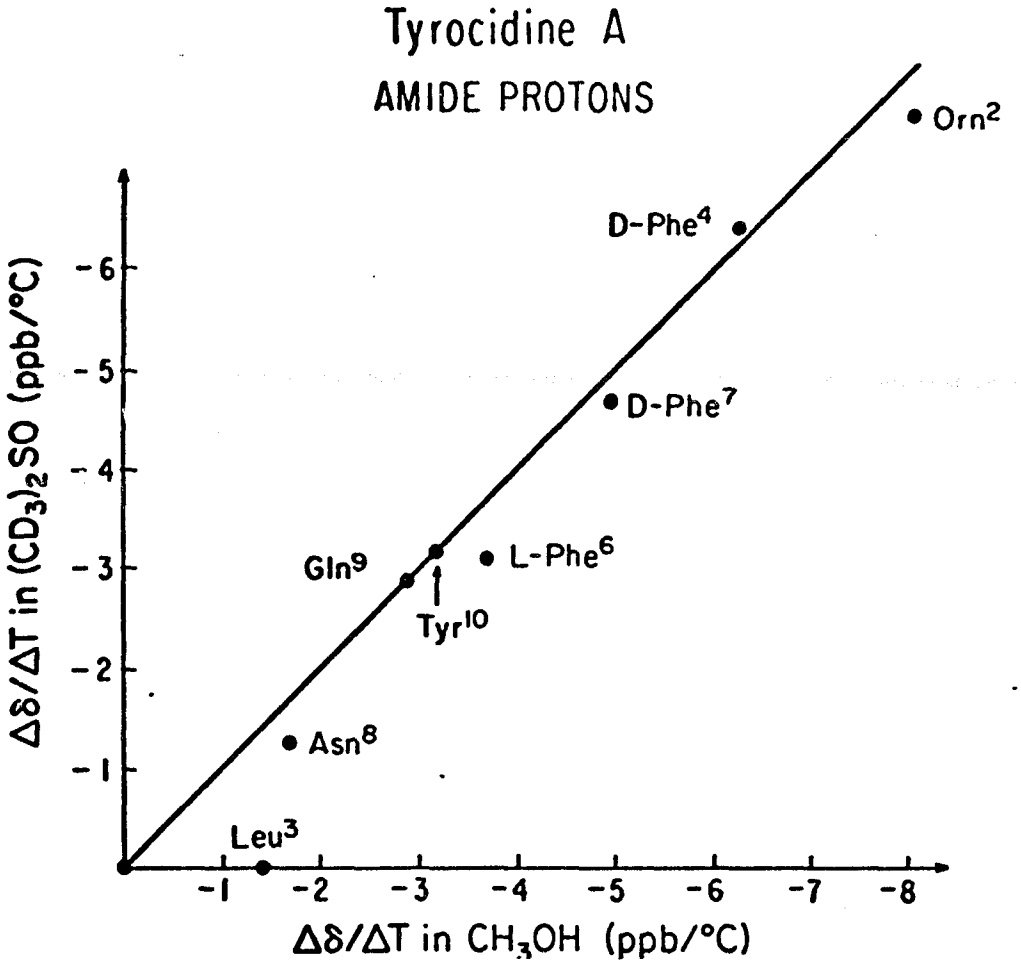

Figure 4

Correlation of the Temperature Dependences of the Chemical Shifts of the Backbone Amide Protons of Tyrocidine A in $(CD_3)_2SO$ and CH_3OH

hydrogen bonding for L-Phe^6, Gln^9 and Tyr^{10}.

b. Hydrogen-Deuterium Exchange Studies

Materials and Methods: Purified tyrocidine A was dissolved in either $(CD_3)_2SO$ or CD_3OD, 25 mg/0.7 ml. In the case of $(CD_3)_2SO$ as the solvent, D_2O was added --$(CD_3)_2SO/D_2O$, 14:1 v/v--to promote exchange. The temperature for the course of the experiment was set at 20-25°C by allowing dry air at room temperature to flow through the spectrometer probe. Spectra of the amide region were obtained in the CW mode. The signal intensity either at the time of addition of D_2O (when $(CD_3)_2SO$ was used as the solvent or at the time of dissolution when CD_3OD was used as the solvent) was taken as the maximum intensity, and the time is arbitrarily designated to be zero. After exchange was commenced, spectra were taken as a function of time.

Results and Discussion: The data are presented in Figures 5 and 6 and summarized in Table II. The maximum intensities were arbitrarily assigned the value of 100 percent, and the intensities as a function of time are expressed as the relative percentage decrease from their maximum values. The experimental error of each measurement of intensity is $\pm$ 10 percent.

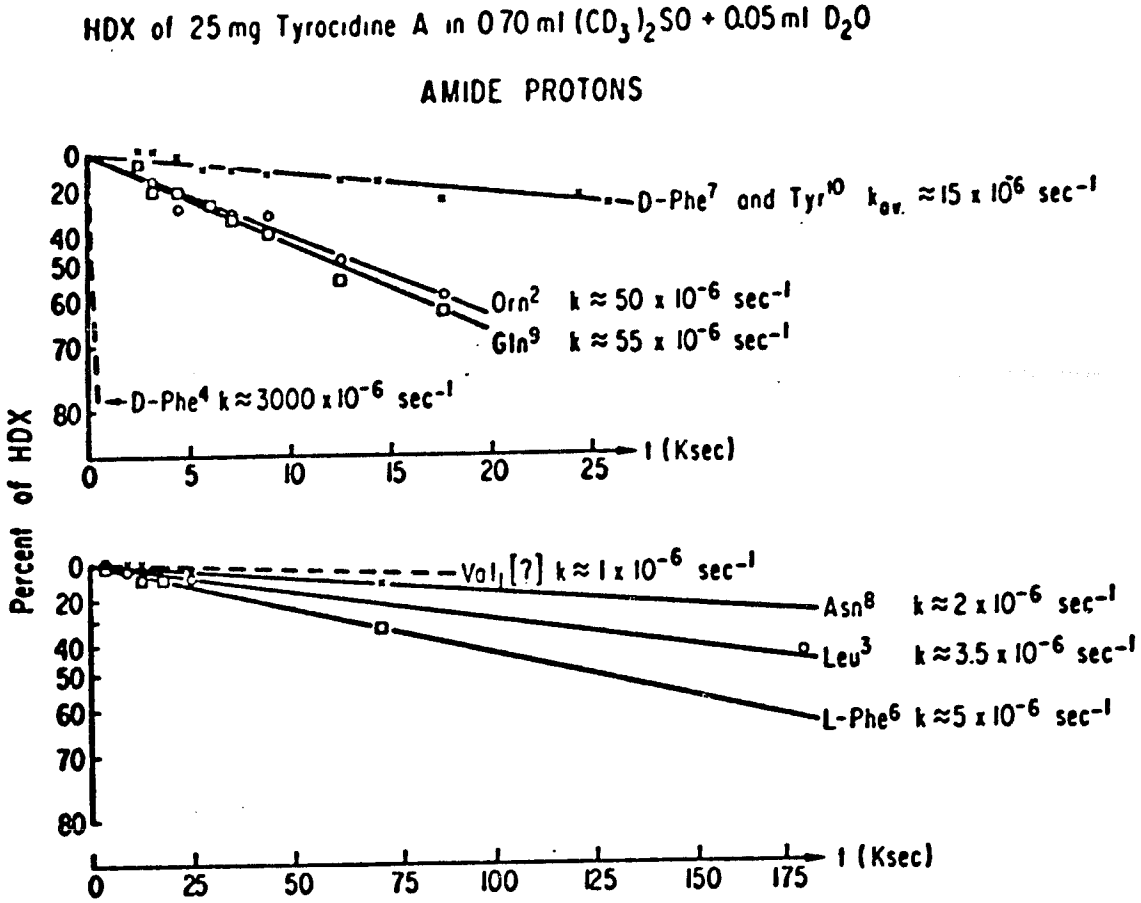

Figure 5

Hydrogen-Deuterium Exchange (HDX) Rates of the Backbone Amide Protons of Tyrocidine A in $(CD_3)_2SO/D_2O$, 14:1 (v/v), at 20-25°C.

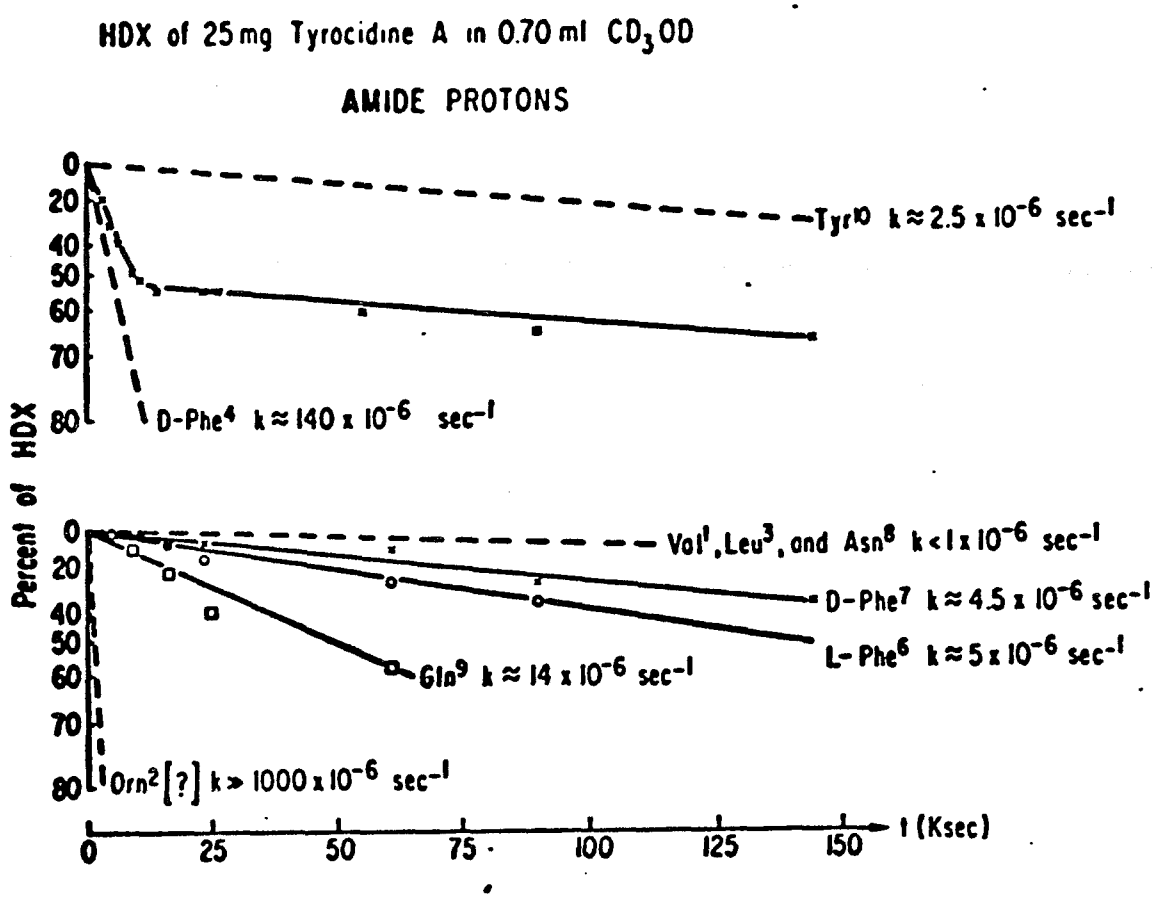

Figure 6

Hydrogen-Deuterium Exchange Rates of the Backbone Amide Protons of Tyrocidine A in CD_3OD at 20-25°C.

Table II

Hydrogen-Deuterium Exchange (HDX) Rate Constants of the Backbone Amide Protons of Tyrocidine A

Residue	$k \times 10^{+6}$ (sec^{-1})	
	$(CD_3)_2SO$	CD_3OD
L-Val[1]	Obscured	<1
L-Orn[2]	50	>>1000
L-Leu[3]	3.5	<1
D-Phe[4]	>3000	140
L-Pro[5]	-	-
L-Phe[6]	5.0	5.0
D-Phe[7]	~15*	4.5**
L-Asn[8]	2.0	<1
L-Gln[9]	55	14
L-Tyr[10]	~15*	2.5**

* Average value (amide proton signals overlap, and individual rates could not be resolved).

**Amide signals overlap, but individual rates could be resolved.

The data from the experiment in which $(CD_3)_2SO/D_2O$ was the solvent fall into two classes corresponding to rapidly and slowly exchanging amide protons. The former class is comprised of the backbone amide protons of Orn^2, D-Phe^4, D-Phe^7, Gln^9 and Tyr^{10}. The resonances of the amide protons of D-Phe^7 and Tyr^{10} overlap and individual rate constants for these two amide protons could not be extracted by data analysis, thereby indicating that their individual rates are relatively close (within a factor of 2 or 3). The slowly exchanging class of backbone amide protons consists of those of Leu^3, L-Phe^6 and Asn^8. Unfortunately, the exchange rate for the amide proton of Val^1 could not be determined because it was obscured by the resonances of the aromatic protons.

In CD_3OD there are again two classes of exchanging protons. The rapidly exchanging class contains the backbone amide protons of Orn^2, D-Phe^4 and Gln^9. The slowly exchanging class can be subdivided into moderately slowly and very slowly exchanging-- $k \geq 1 \times 10^{-6}$ sec^{-1} and $k < 1 \times 10^{-6}$ sec^{-1}, respectively. By this arbitrary division, the backbone amide protons of L-Phe^6, D-Phe^7 and Tyr^{10} form the moderately slow subdivision and those of Val^1, Leu^3 and Asn^8 comprise the very slow subclass.

Inspection of the data in Table II indicates that the backbone amide protons of Orn^2, D-Phe^4 and Gln^9 are freely accessible to the solvent--i.e., not intramolecularly hydrogen-bonded--in both solvent systems. The backbone amide protons of Val^1, Leu^3 and Asn^8, which have the smallest exchange rate, are intramolecularly hydrogen-bonded and not readily available to interaction with solvent. The amide protons of L-Phe^6, D-Phe^7 and Tyr^{10} possess borderline HDX rates. The behavior of the amide protons of D-Phe^7 and Tyr^{10} in $(CD_3)_2SO/D_2O$ is consistent with their being sterically shielded from the solvent, rather than with their involvement in intramolecular hydrogen bonding. The amide proton of L-Phe^6 may be participating in a "weak" intramolecular hydrogen bond.

Comparison of the temperature-dependence data with the HDX studies gives good correlation for intramolecular hydrogen bonding of the backbone amide protons of Val^1, Leu^3 and Asn^8. By the criteria of HDX, the backbone amide proton of Gln^9 cannot be hydrogen bonded; therefore, temperature perturbations must activate a mechanism which leads to a decreased interaction of the backbone amide proton of Gln^9 with solvent. A possible mechanism that could produce this effect would be thermal

activation of side chain rotation leading to a change in the average rotomer populations. Inspection of a CPK model for the proposed structure of tyrocidine A shows that the backbone amide proton of Gln^9 can be sterically blocked from solvent by its own side chain as well as the side chain of Asn^8. Thus, the anomalous behavior of the backbone amide proton--i.e., fast exchange rate and low temperature dependence--may be a reflection of different rotomer populations at different temperatures.

A similar mechanism may be operative in the case of the amide proton of D-Phe^7. At lower temperatures this proton would be sterically hindered from solvent interactions, leading to a lowered exchange rate. As a function of temperature this amide proton would become relatively more solvent exposed because of changing rotomer populations; therefore, it exhibits a borderline exchange rate and high temperature dependence.

The amide protons of L-Phe^6 and Tyr^{10} are difficult to characterize on the basis of temperature-dependence and HDX studies since they yield borderline behavior by both criteria. Consideration of a CPK model for the proposed structure of tyrocidine A, however, indicates that steric hindrance may be the source of the behavior of the amide proton of Tyr^{10} and that the amide proton

of L-Phe[6] appears to be involved in the formation of a transannular hydrogen bond.

c. Solvent Perturbation of the Chemical Shifts of the Amide Protons

Materials and Methods: Purified tyrocidine A was dissolved in CH_3OH and also in $(CD_3)_2SO$, 25 mg/0.7 ml, each containing TMS as an internal reference.

The spectrometer was operated in the CW mode. To minimize spectral overlap the temperature was maintained at $65^oC \pm 2^oC$.

The sample dissolved in CH_3OH was titrated with additions of $(CD_3)_2SO$, and the sample dissolved in $(CD_3)_2SO$ was titrated with additions of CH_3OH until each sample achieved a 55 volume percent composition of the titrant. Upon each addition of titrant spectra were recorded in sections 500-Hz wide.

Results and Discussion: Inspection of the data presented in Figure 7 reveals that in response to increasing solvent polarity, CH_3OH to $(CD_3)_2SO$ ($\epsilon = 33.6$ to $\epsilon = 46.6$), the amide protons exhibit two classes of behavior and fall into two groups of chemical shifts. In one class the chemical shift is a monotonic function of solvent polarity. This class consists of

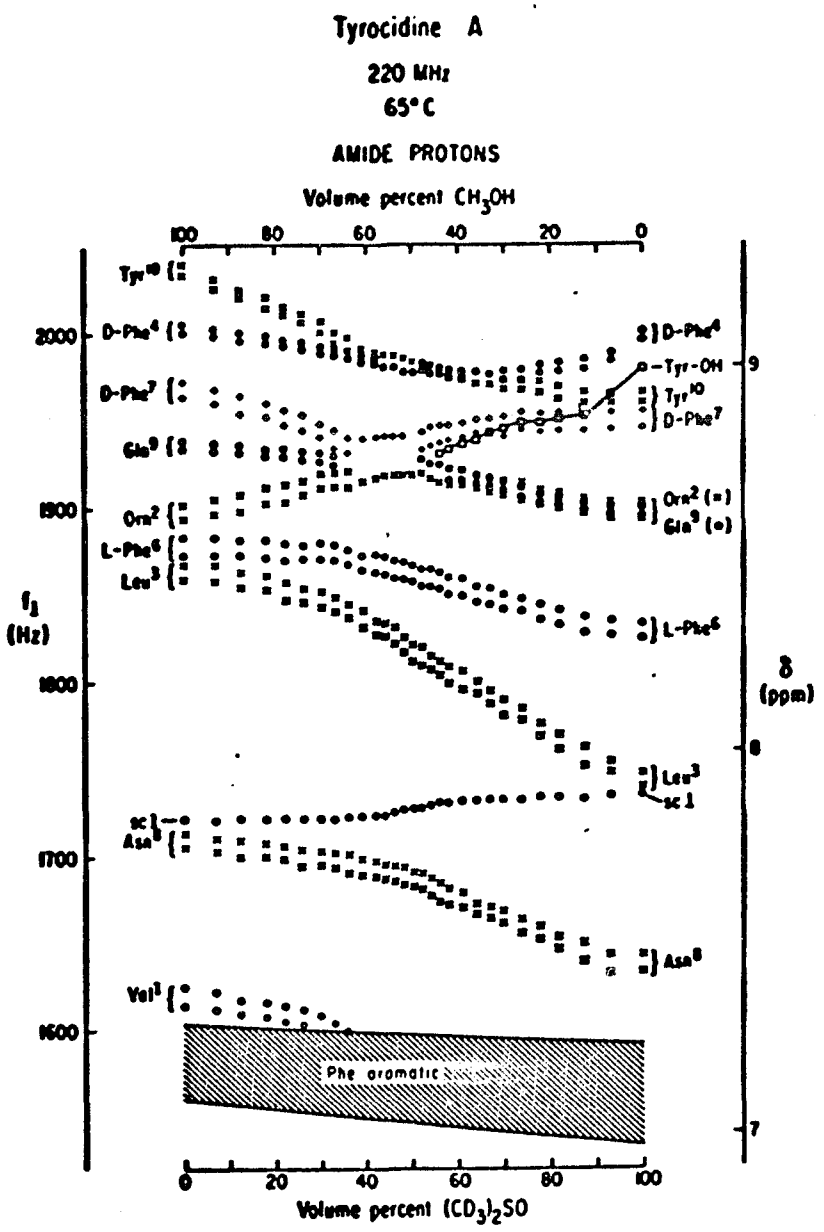

Figure 7

Solvent Perturbation of the Amide Protons of Tyrocidine A at 65° ± 2°C.

the amide protons of Val[1], Leu[3], D-Phe[4], L-Phe[6], Asn[8], Gln[9] and Tyr[10]. The non-monotonic class contains the amide protons of Orn[2] and D-Phe[7].

A possible explanation for the behavior of this latter class of protons may be related to the reorientation of side chains, either their own or of adjacent residues, as a function of solvent polarity. Some support for this hypothesis is given by a preliminary water-titration experiment. In this study, 20 mg of tyrocidine A was dissolved in 0.7 ml of $(CD_3)_2SO$. The probe was maintained at ambient temperature (20-25°C) to eliminate exchange-broadening of the amide proton resonances. The sample was titrated with H_2O (ϵ = 80.4) to 20 volume percent (line-broadening indicated the beginning of water-induced aggregation at the upper level of water content achieved). By the criteria of both temperature dependence of the chemical shifts and HDX rates, the D-Phe[4] amide proton and the Tyr[10] side-chain OH proton are both solvent exposed. Thus, as a function of increasing solvent polarity, these protons should, in the absence of other effects, both shift downfield--i.e., water should form more and/or stronger hydrogen bonds than $(CD_3)_2SO$, thereby leading to more deshielding (downfield shift) of these protons in the former solvent.

Over the range of water titration, the Tyr^{10} OH proton executed a monotonic, downfield shift of 30 Hz (0.14 ppm), while the amide proton of D-Phe^{4} shifted monotonically upfield by 10 Hz (0.05 ppm).

The anomalous upfield shift is consistent with changes in the rotomer populations of the D-Phe^{4} side chain so as to increase the diamagnetic field of the D-Phe^{4} amide proton--i.e., the upfield shifts that resulted from changes in the rotomer populations overwhelmed the downfield shifts that should have been produced by the solvent titration per se. It is therefore conceivable that the Orn^{2} and D-Phe^{7} amide proton behavior can be rationalized on the basis of their response to changing solvent polarity superimposed upon a change in rotomer populations of their own or neighboring side chains.

The vicinal amide-C^{α} proton coupling constants are the same ($\pm$ 0.5 Hz) in both solvents. On the basis of this observation it may be concluded that the backbone conformation does not undergo any changes in going from one solvent to the other that could be detected by nmr. It is possible, but highly unlikely, that the secondary structure could change and attain ϕ and ψ angles which would yield identical coupling constants for the eight

amide protons visible in both solvents.

The general behavior of the chemical shifts of the amide protons in response to increasing solvent polarity falls into two groups based on the direction of their shifts. In the absence of other effects, the amide protons of the upfield-shifted group are involved in the formation of intramolecular hydrogen bonds, while those in the downfield-shifted group are solvent exposed, for the reasons previously discussed. By these criteria, the backbone amide protons of Val^1, Leu^3, and Asn^8 are clearly intramolecularly hydrogen-bonded, while those of L-Phe^6 and Tyr^{10} may be intramolecularly hydrogen-bonded. The downfield-shifted backbone amide protons of Orn^2, D-Phe^4, D-Phe^7 and Gln^9 are solvent exposed --hence, not intramolecularly hydrogen-bonded.

When the data for temperature dependence, HDX and solvent perturbations are considered in total, the following picture emerges: There are unequivocally three intramolecularly hydrogen-bonded backbone amide protons --viz., those of Val^1, Leu^3 and Asn^8. The four backbone amide protons of Orn^2, D-Phe^4, D-Phe^7 and Gln^9 are solvent exposed and hence not intramolecularly hydrogen-bonded. The amide protons assigned to L-Phe^6 and Tyr^{10} are borderline by all criteria.

3. Coupling Constant Analysis and Analogy with Gramicidin S

The dihedral angles ϕ, ψ and ω completely specify the conformation of a peptide backbone (3). Conformation about the N-C^{α} bond determines ϕ, about the C^{α}-carbonyl carbon (C^{α}-C') bond determines ψ and about the bond between the carbonyl carbon to the amide nitrogen of the next residue determines ω. These angles are illustrated in Figure 8. The peptide bond is assumed to be planar and the amide hydrogen trans to the carbonyl oxygen. This configuration is characterized by a value for ω of 180^{o}. The Karplus-Bystrov relationship relates the value of the coupling constant, J, between the amide proton and its vicinal C^{α} proton to the dihedral angle ϕ. Hence, by measuring J from the amide proton region of the pmr spectrum, correcting it for the electronegativity of the substituents on the C^{α} atom and substituting this corrected value into the Karplus relationship, ϕ can be obtained. The Karplus relationship is given as follows:

$$J^{\text{corrected}} = A \cos^2\theta - B \cos\theta + C \sin^2\theta$$

where θ is the dihedral angle between the H-N and C^{α}-H planes.

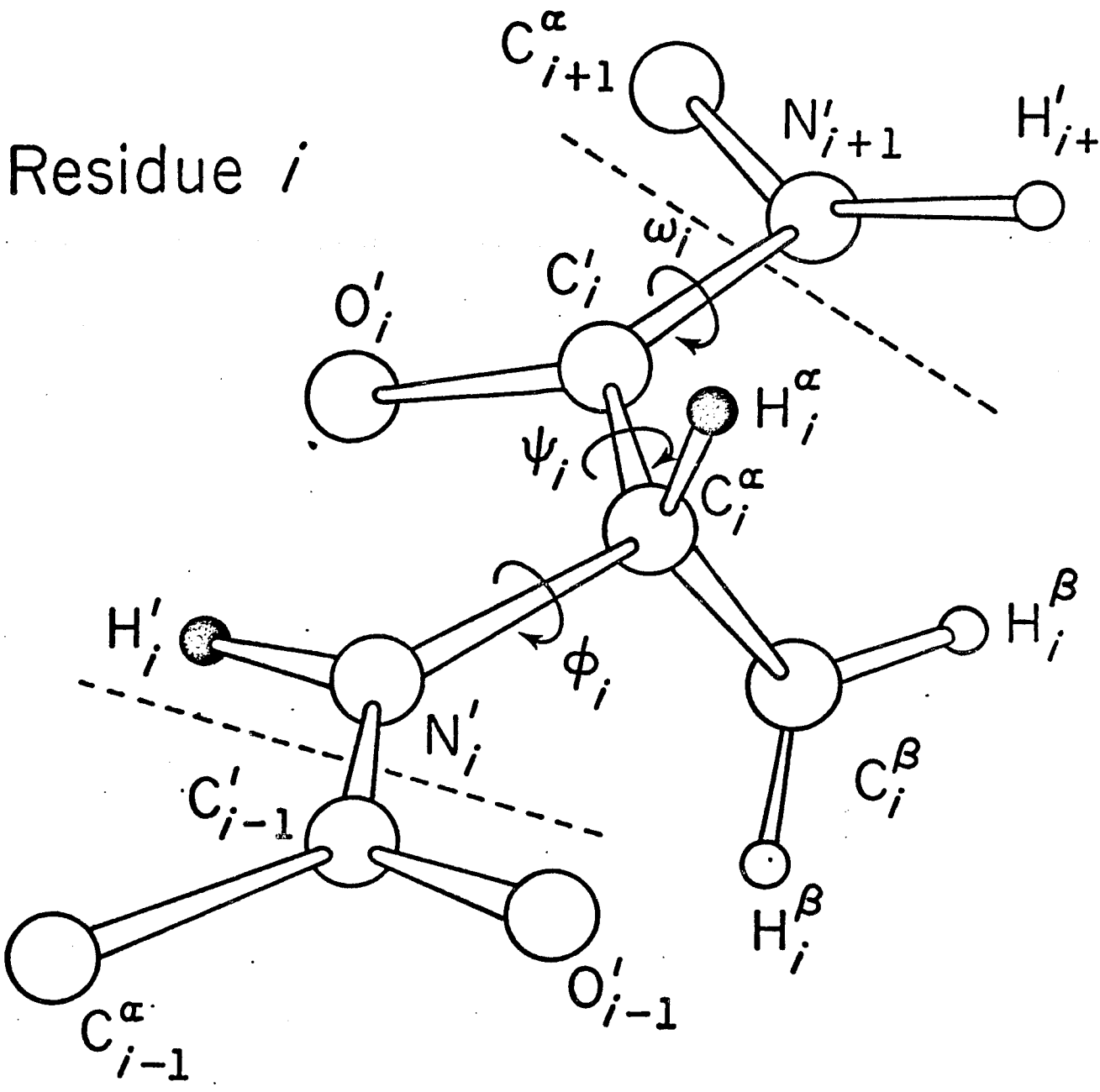

Figure 8

Designation of the Dihedral Angles ϕ, ψ, and ω of a Peptide Backbone

(By definition, $\theta = 0^{o}$ when the amide proton and the C^{α} proton are cis. When this obtains, then $\phi = 60^{o}$ (3).

Bystrov et al. (37, 38) have proposed that A = 9.8 Hz, B = 1.1 Hz and C = 0.4 Hz and that $J^{corrected} = 1.09 \times J^{observed}$ for all residues except the glycyl residue, for which $J^{corrected} = 1.04 \times J^{observed}$.

There is no way to obtain the angle ψ directly from proton-proton spin couplings. Determination of this dihedral angle requires the measurement of the hetero-nuclear coupling constant between the C^{α} proton of one residue and a ^{15}N-enriched amide nitrogen of the adjacent residue (37, 38, 45). Reasonable values of the angle ψ, however, can be estimated from ϕ by making some assumption as to the secondary structure. By virtue of the homology of residues one through five between gramicidin S and tyrocidine A and the coupling constant J of D-Phe^{4}, it seems reasonable that tyrocidine A should approximate a β-pleated sheet structure similar to that of gramicidin S. On this assumption, the dihedral angle ψ was calculated for each residue.

The calculated values of ϕ and ψ, presented in Table III, can be related to a Ramachandran plot, which relates

Table III

Vicinal Amide-C^{α} Proton Coupling Constants (J) and the Proposed Backbone Dihedral Angles ϕ and ψ of Tyrocidine A in $(CD_3)_2SO$ at 51°C

Residue	$J^{observed}$ (Hz)	$J^{corrected}$ (Hz)	ϕ*	ψ*
L-Val[1]	-	-	-142.5°**	+137.5°**
L-Orn[2]	8.6	9.4	-142.5°	+137.5°
L-Leu[3]	8.5	9.3	-95°	+137.5°
D-Phe[4]	2.4	2.6	-5°	-47.5°
L-Pro[5]	-	-	-60°**	-32.5°**
L-Phe[6]	10.0	10.9	-120°	+115°
D-Phe[7]	8.7	9.5	+ 97.5°	-90°
L-Asn[8]	8.5	-	-142.5°	+137.5°
L-Gln[9]	2.7	2.9	- 7.5°	-57.5°
L-Tyr[10]	7.2	7.9	-85°	-10°

* 1970 IUPAC convention (3).

**Based on analogy with these parameters in gramicidin S (61).

the dihedral angles to the conformational energy (45, 46). From this plot the conformational energy related to any given pair of angles can be estimated. A calculation of the dihedral angles obtained for tyrocidine A placed six of the ten residues in the region of energy minima. The residues of D-Phe^4, D-Phe^7, Gln^9 and Tyr^{10} fall outside the minima boundaries. This is similar to the findings reported for the crystal conformation of the sodium complex of the cyclic decapeptide antaminide (47). This cyclic peptide also contained four deviant residues. These deviations may reflect constraints set by the cyclic structures of the backbones of these molecules.

Comparison of the spectral parameters of tyrocidine A with those of gramicidin S--both in $(CD_3)_2SO$--reveals some striking similarities. For both, the most downfield resonance is that of the D-Phe^4 amide proton; in addition to their chemical shifts, their coupling constants are virtually identical. The D-residue with its small coupling constant is consistent with a dihedral angle ϕ that corresponds to a cis arrangement of the two C' atoms adjacent to the N-C$^\alpha$ bond. Additionally, since this residue is linked to Pro^5, by analogy with gramicidin S, residues four and five form a β-turn.

Gln^9 is the other residue whose amide proton possesses a small coupling constant. Scheraga, by considering the energy of the side chain backbone interactions, has classed glutamine among those amino acids capable of generating an α-helix (48). Based on consideration of the magnitude of the coupling constant and the temperature dependence, however, Gln^9 was placed in the first corner position in a β-turn. Therefore, Tyr^{10} would occupy the second corner position of this β-turn.

Since a β-turn usually involves a four-fragment residue (with the two corner residues occupying the inner positions), the tetrapeptide moieties Leu^3-D-Phe^4-Pro^5-L-Phe^6 and Asn^8-Gln^9-Tyr^{10}-Val^1 are those involved in executing the β-turns.

Based on the above considerations, a CPK model containing these β-turns and having dihedral angles as determined by the coupling constants was constructed. The model is shown in Figure 9.

The resultant structure is an antiparallel β-pleated sheet containing three planar intramolecular transannular hydrogen bonds--viz., those formed by the backbone amide protons of Val^1, Leu^3 and Asn^8--and one intramolecular hydrogen bond slightly out of the plane of the backbone --viz., that formed by the amide proton of L-Phe^6.

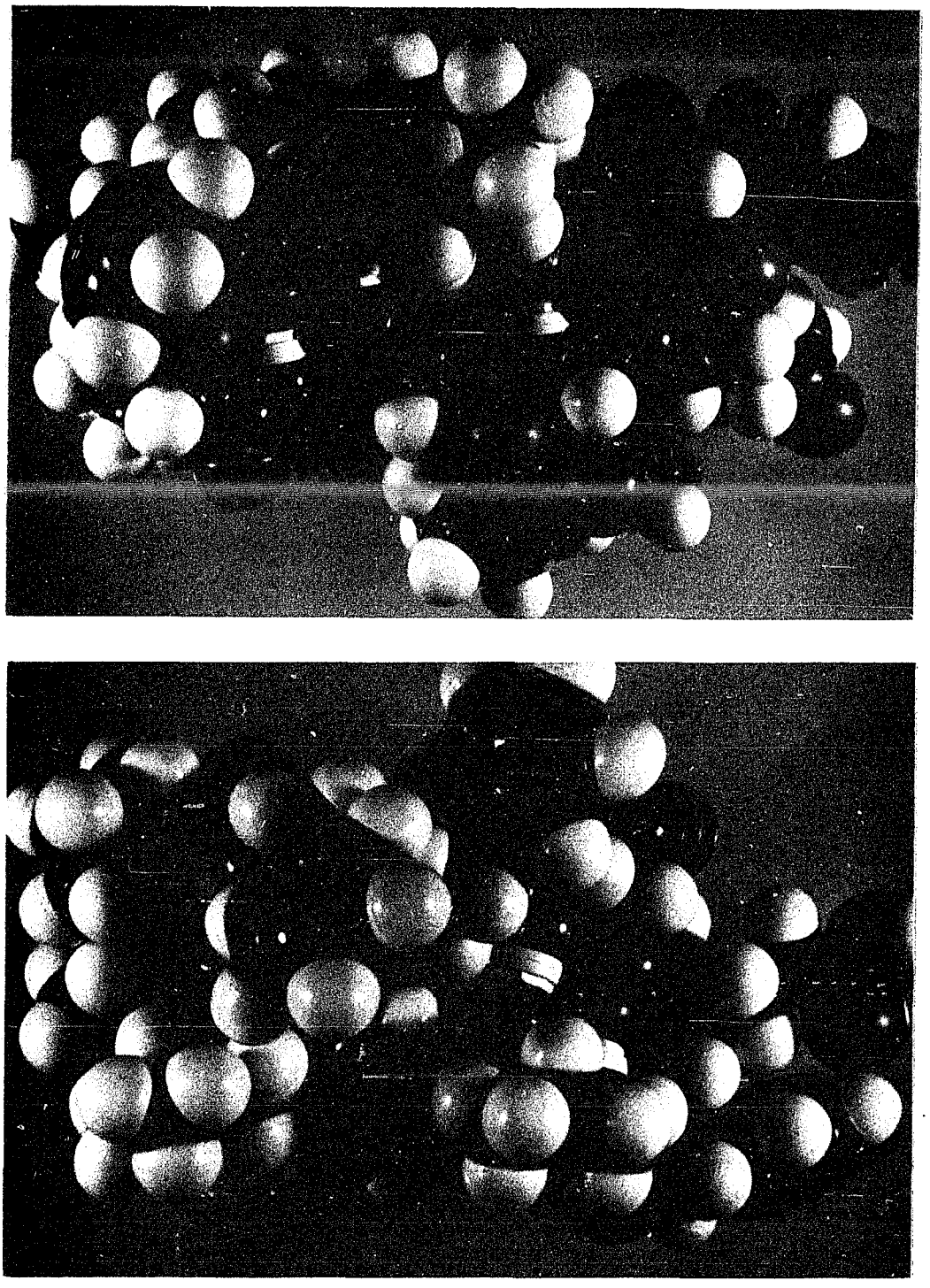

Figure 9

CPK Model for the Proposed Secondary Structure of Tyrocidine A. Upper photograph depicts the arbitrarily designated upper surfac of the molecule; lower photograph depicts the lower surface of the molecule.

Black = Carbon atoms Red = Oxygen atoms
Blue = Nitrogen atoms White = Hydrogen atoms
Orientation: D-Phe^{4}-Pro^{5} β-turn on the left;
Gln^{9}-Tyr^{10} β-turn on the right.

The C^{α} proton of D-Phe^{7} is below the plane of the ring. The anomalously downfield chemical shifts of the Orn^{2} and D-Phe^{7} C^{α} protons can be rationalized, at least in part, as caused by magnetic anisotropy due to the presence of the aromatic rings (49). Thus, the D-Phe^{7} C^{α} proton is shifted by its own side chain and/or the side chain of the L-Phe^{6}, while the C^{α} proton of Orn^{2} is influenced by the orientation of the side chain of L-Phe^{6} beneath the plane of the ring.

The amide protons of Orn^{2}, D-Phe^{4} and D-Phe^{7} are solvent exposed and sterically unhindered. The amide protons of Gln^{9} and Tyr^{10} are solvent exposed but shielded by their own as well as adjacent side chains.

It is conceivable that the Gln^{9} amide proton may hydrogen-bond with the carboxamide oxygen atom in the side chain of Asn^{8}, but there is no direct proof for this speculation.

The side chains of Orn^{2}, D-Phe^{4} and Tyr^{10} all point above[5] the plane of the ring formed by the backbone, while those of D-Phe^{7}, Asn^{8} and Gln^{9} are oriented to the side and slightly below this plane; the remaining side chains

---

5. The designations "above" and below" the plane are arbitrary.

are below this plane. Additionally, most of the polar residues are clustered around the Gln^9-Tyr^{10} β-turn. Viewing this molecule from the top (Figure 9), one sees Orn^2, Tyr^{10}, Gln^9 and Asn^8. The side chains of Val^1, Leu^3 and L-Phe^6 are located below the plane of the ring away from the polar side chains.

Although it is assumed that gramicidin S and tyrocidine A manifest similar backbone conformations in that both possess antiparallel β-pleated sheets connected by two β-turns, gramicidin S appears to be a much more tightly packed molecule with respect to its sheet structure than tyrocidine A. More importantly, the two ornithyl side chains lie across the top of the backbone ring, effectively occluding the plane formed by the β-pleated sheet of the backbone. In the proposed conformation of tyrocidine A, however, this occlusion does not occur, and a good portion of the β-pleated sheet structure is available for intermolecular interactions.

Thus, based on this postulated conformation, consistent with the nmr parameters obtained, it was feasible to undertake a study of the aggregation process by nmr.

CHAPTER III

AGGREGATION STUDIES

A. General Discussion

Nmr parameters which can be used as indexes of aggregation are:

(i) Changes in proton chemical shifts (not due to temperature).

(ii) Changes in line widths (T_2 mechanisms).

(iii) Changes in spin-lattice relaxation times (T_1 processes).

(iv) Changes in coupling constants (conformational changes).

Of the above parameters, (i) and (ii) are the most easily measured and subject to the least experimental error. Interpretation of spin-lattice relaxation time measurements for protons are in general not straightforward. Protons, being on the exterior of a molecule, are subject to interactions with solvent molecules as well as neighboring groups on the same or nearby solute molecules, and this rate of relaxation is a function of the motion of the group to which they are bonded, the overall motion of molecule in which they reside, and interactions with neighboring molecules of the same

species (50-53).

Changes in coupling constants would provide useful structural information. These changes, however, are difficult to extract when the spectra are broadened due to the aggregation process or when the region observed, such as the C^{β} proton region of aromatic residues, does not consist of first-order spin systems--i.e., the differences in the chemical shifts of the coupled protons are of the same magnitude as the coupling constants themselves. Thus, although these changes may be occurring, they are obscured by other factors and cannot be quantified.

The determination of the chemical shift and the line width of a resonance signal is generally straightforward and can be achieved for most of the amide and C^{α} protons in peptide spectra. Even when spectral overlap occurs, it is still often possible to extract the chemical shifts of these particular protons visually; the line widths, however, cannot be extracted by this means.

Changes in the chemical shift of a particular proton (at constant temperature) can be due to changes in its interaction with solvent--e.g., hydrogen bonding to solvent--changes in its exchange rate with other protons (either solvent or solute protons) or exposure to magnetically anisotropic species. All of these factors can

lead to changes in the shielding about a proton and, thus, the energy of irradiation it requires to achieve resonance.

Increased interaction of a proton with a good hydrogen bond-forming solvent produces downfield shifts, while a decreased interaction leads to upfield shifts. As stated earlier, these shifts are ultimately due to the relatively deshielded state of a proton participating in a hydrogen bond.

In the case of an exchanging proton, the observed chemical shift can, under certain conditions, be a function of the rates of exchange and of the two magnetic sites or environments experienced by that proton--i.e., the environment in the solvent as well as in the peptide. If the rate of exchange is slow compared to the time the proton spends at each site, two distinct signals corresponding to each site may be observed. As the rate of exchange increases, the signals begin to move toward each other and broaden. At very fast exchange rates, only one sharp signal is observed whose apparent chemical shift is a weighted average of the chemical shifts at the two sites; each weight is proportional to the average lifetime at the site (54). Thus, for a solvent-exposed amide proton exchanging with protons from residual acid that contaminates the solvent (see Chapter III, Section B

for the source of this contamination), one site would be located in the peptide and the other in the solvent. As the rate of exchange increases, the fraction of populations at the two sites change in favor of the location in the solvent, the proton is more deshielded at the solvent site than at the peptide site, then the observed resonance would move downfield as equilibrium is shifted to the solvent site by the addition of more acid.

Changes in chemical shifts brought about by magnetically anisotropic groups are a function of both the orientation and the distance of the perturbing groups relative to the affected proton. In peptides, carbonyl oxygens and side chains of aromatic residues are examples of groups capable of producing anisotropic shifts on protons. The amount of chemical shift these groups can produce as functions of their distance and orientation are well established (49). Thus, it is possible to work from the observed shift of a proton and extract compatible distances and orientations of the perturbing group.

All other things being equal, increasing concentrations of gramicidin S and tyrocidine A should give rise to different spectral characteristics inasmuch as tyrocidine A but not gramicidin S should begin to aggregate. By analyzing the spectral changes occurring in the control

peptide gramicidin S, qualitative estimates of changes in viscosity and the "acidification" of $(CD_3)_2SO$ produced by increasing peptide concentration could be obtained. These "non-specific" changes unrelated to aggregation per se could then be applied to the tyrocidine A studies to obtain the net effects of aggregation by difference. Thus, the changes in chemical shift produced by variations in exchange rate could be distinguished from chemical shifts produced by magnetically anisotropic residues. Chemical shifts from this latter group would then provide information about quaternary structure in the aggregate.

B. Aggregation Studies on Gramicidin S and Tyrocidine A

Materials and Methods: Purified tyrocidine A and gramicidin S were each dissolved in $(CD_3)_2SO$, 200 mg/0.7 ml and 100 mg/0.7 ml, respectively. TMS was used as an internal reference. Dilutions were made by removing an aliquot of sample and replacing it with an equal aliquot of solvent. Spectra were obtained at each concentration.

The spectrometer was operated in the Fourier transform mode (ftnmr). The final 2500-Hz sweep width spectrum was distributed over 4096 points in the dedicated computer attached to the spectrometer. This distribution gives an intrinsic resolution of 0.61 Hz/point. On this basis,

chemical shifts and line width determinations have an inherent error of not less than ±0.61 Hz. Practical considerations of line broadening and signal overlap would yield an experimental error of ±2 Hz (0.01 ppm).

Results and Discussion: The chemical shifts of the protons at each concentration for the control peptide gramicidin S are presented in Figures 10 and 11. Over a ten-fold concentration range, the chemical shifts of all protons except the D-Phe^4 amide proton are remarkably independent of the concentration. In addition, as can be seen from Figure 12, the line widths of the gramicidin S amide protons do not change appreciably at the two extreme concentrations.

These spectral characteristics should be contrasted with the chemical shift behavior of the tyrocidine A protons, Figures 13 through 16, and the line width changes evident in Figure 17. Examination of the chemical shifts of the amide regions of gramicidin S and tyrocidine A (Figures 10 and 13) indicate that the behavior of the D-Phe^4 amide proton is similar in both compounds and, therefore, may be unrelated to the aggregation process.

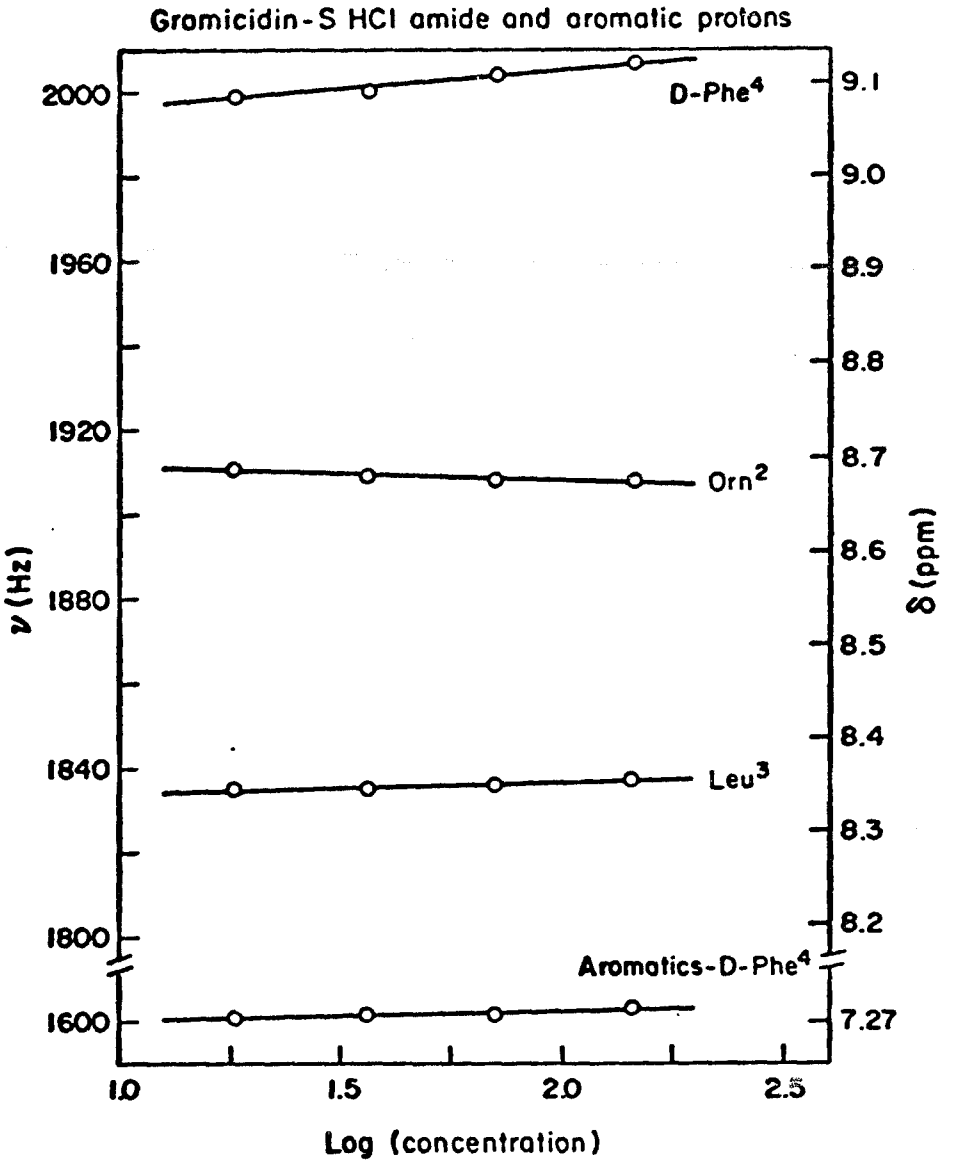

Figure 10

Chemical Shifts of the Amide Protons of Gramicidin S in $(CD_3)_2SO$ at $28^{\circ} \pm 2^{\circ}C$ as a Function of Concentration (mg/ml).

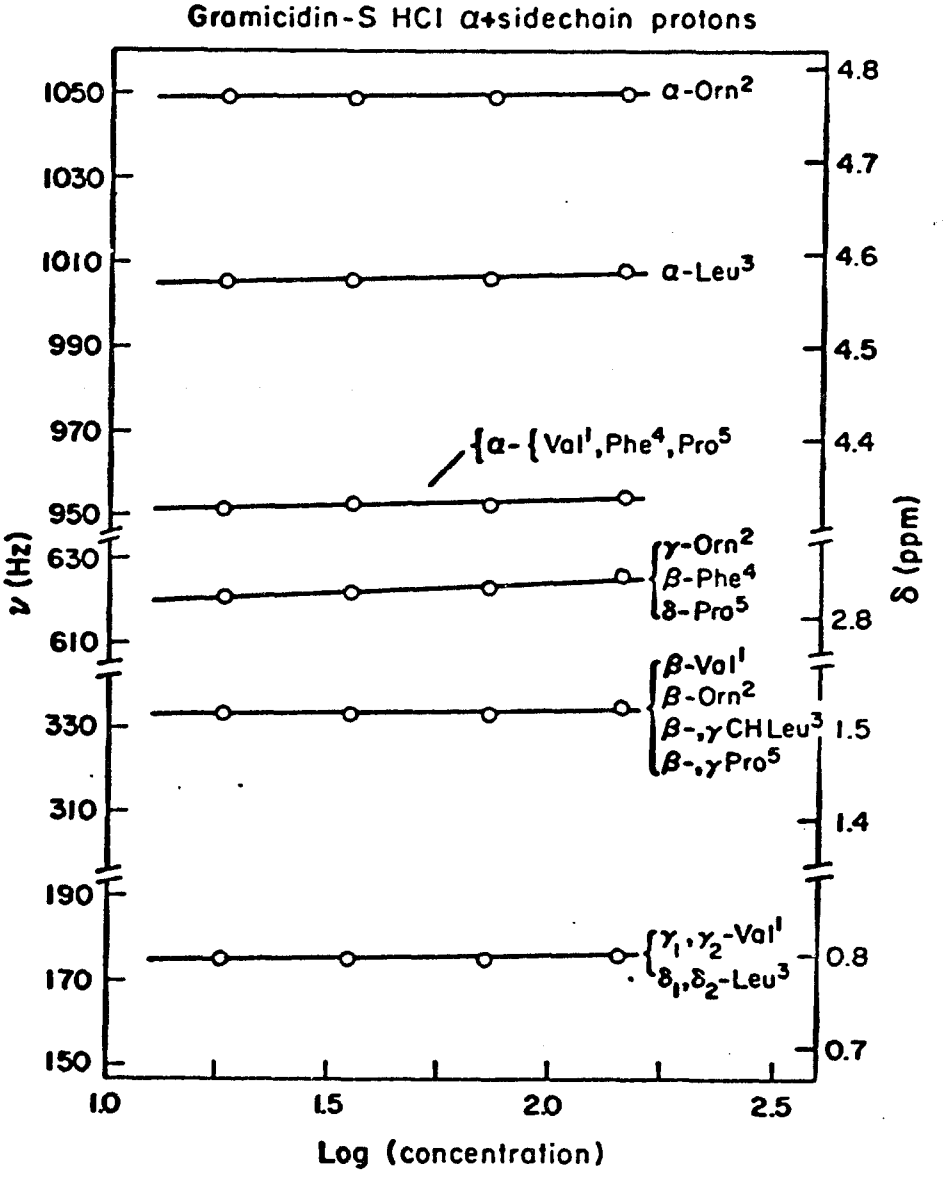

Figure 11

Chemical Shifts of the C^{α} and Side-Chain Protons of Gramicidin S in $(CD_3)_2SO$ at $28^{o} \pm 2^{o}C$ as a Function of Concentration (mg/ml).

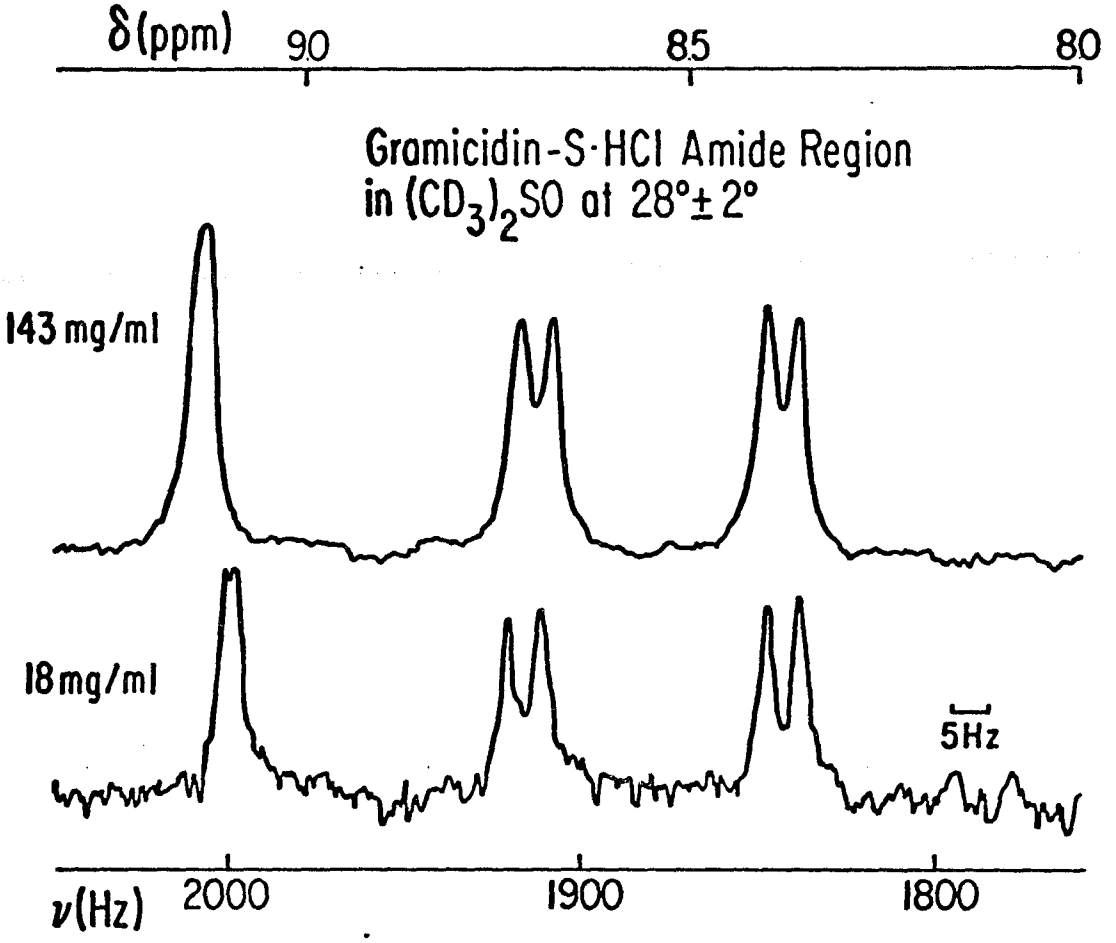

Figure 12

500-Hz Sweep Width Spectra of the Amide Protons of Gramicidin S in $(CD_3)_2SO$ at $28^o \pm 2^oC$ at the Upper and Lower Concentrations for Comparison of Line Widths.

Assignments (left to right): D-Phe^4, Orn^2, Leu^3.

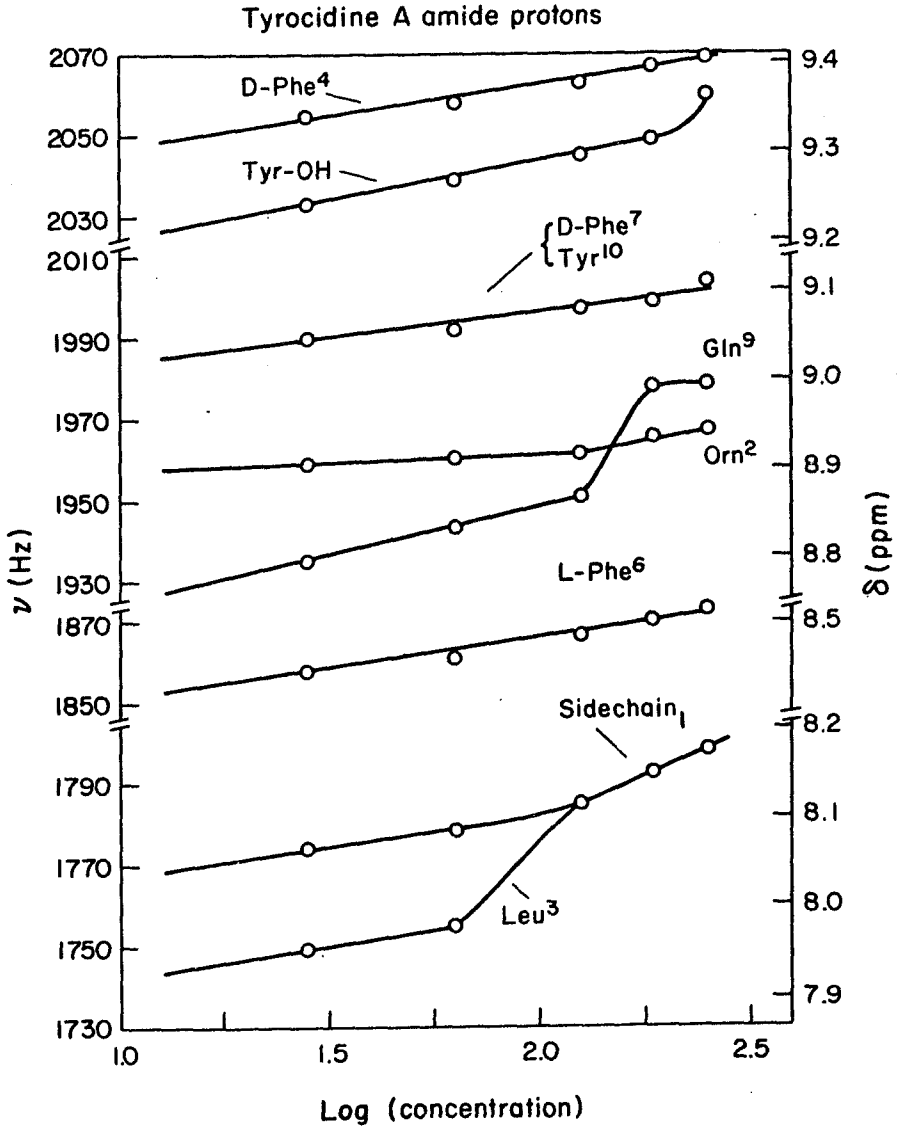

Figure 13

Chemical Shifts of the Amide Protons of Tyrocidine A in $(CD_3)_2SO$ at $20^o \pm 2^oC$ as a Function of Concentration (mg/ml).

NOTE: The chemical shift of the ornithyl δ-NH_3^+ group is not shown.

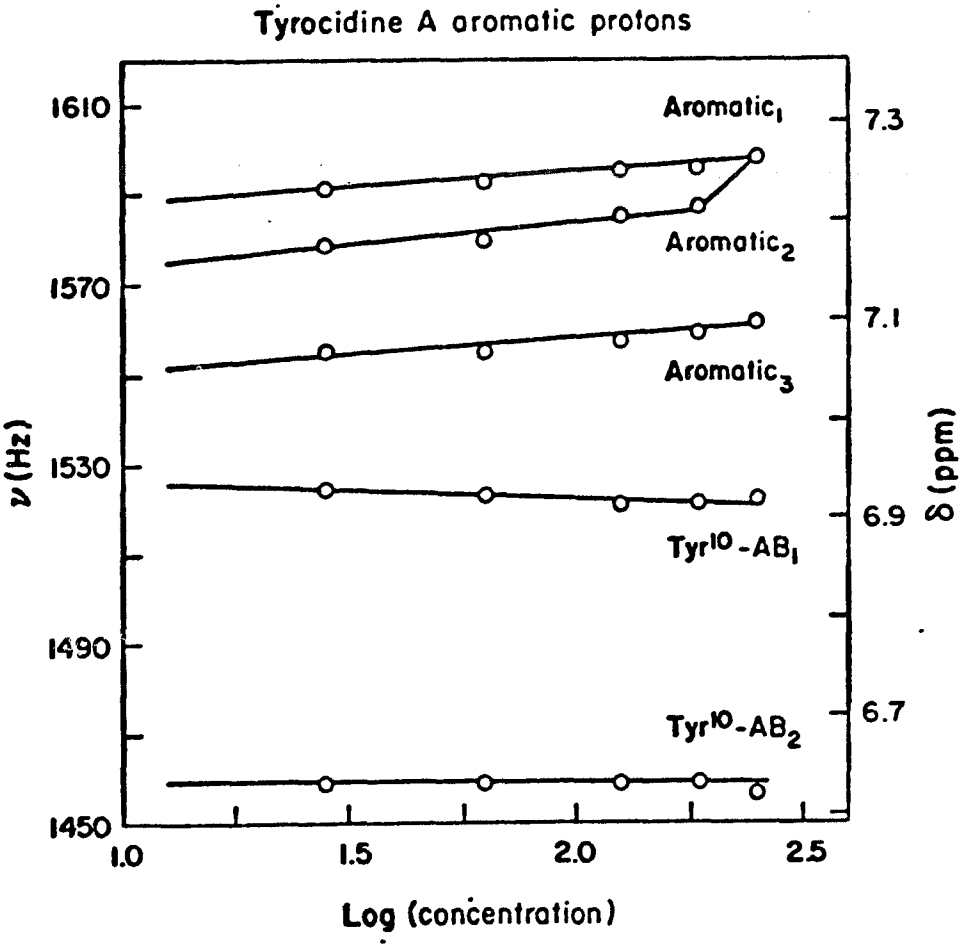

Figure 14

Chemical Shifts of the Aromatic Protons of Tyrocidine A in $(CD_3)_2SO$ at 20° ± 2°C as a Function of Concentration (mg/ml).

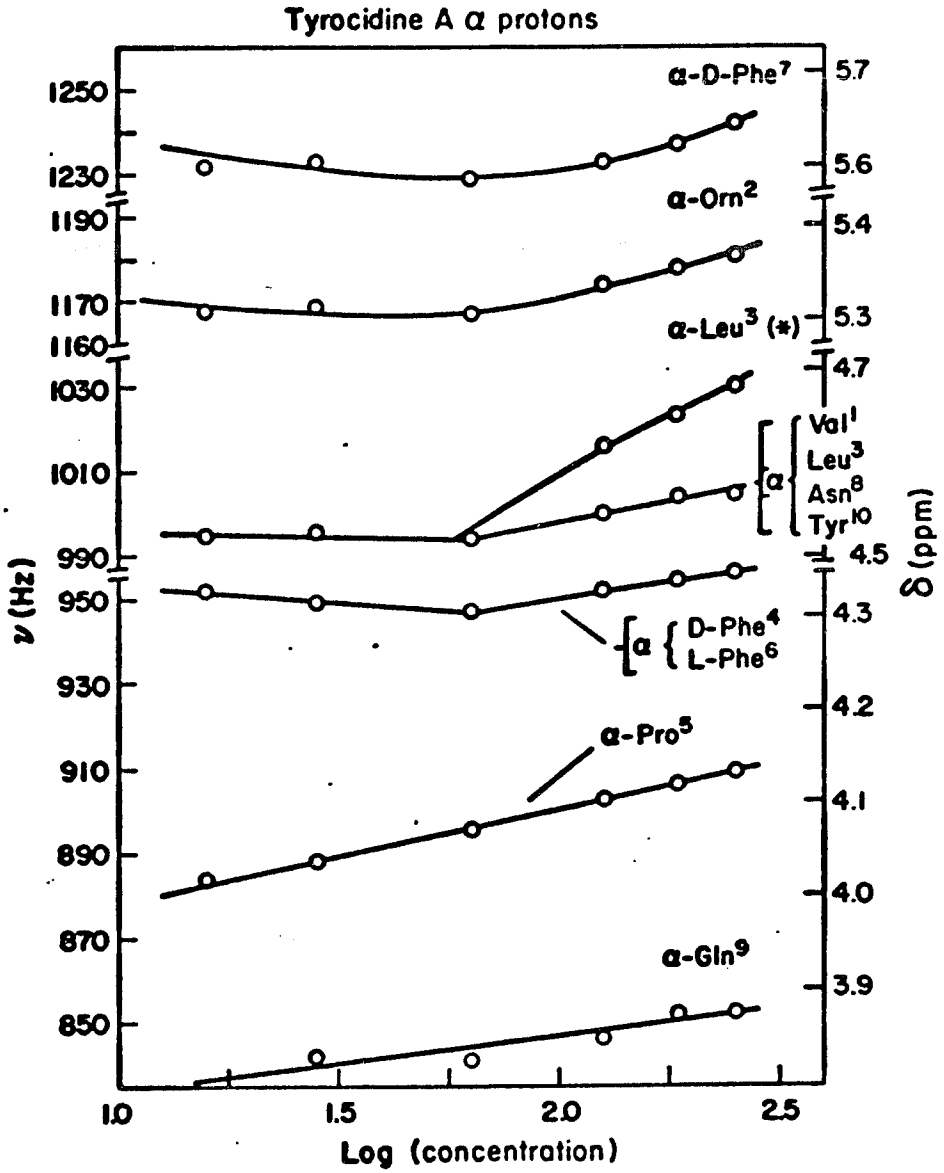

Figure 15

Chemical Shifts of the C^{α} Protons of Tyrocidine A in $(CD_3)_2SO$ at $20^{\circ} \pm 2^{\circ}C$ as a Function of Concentration (mg/ml).

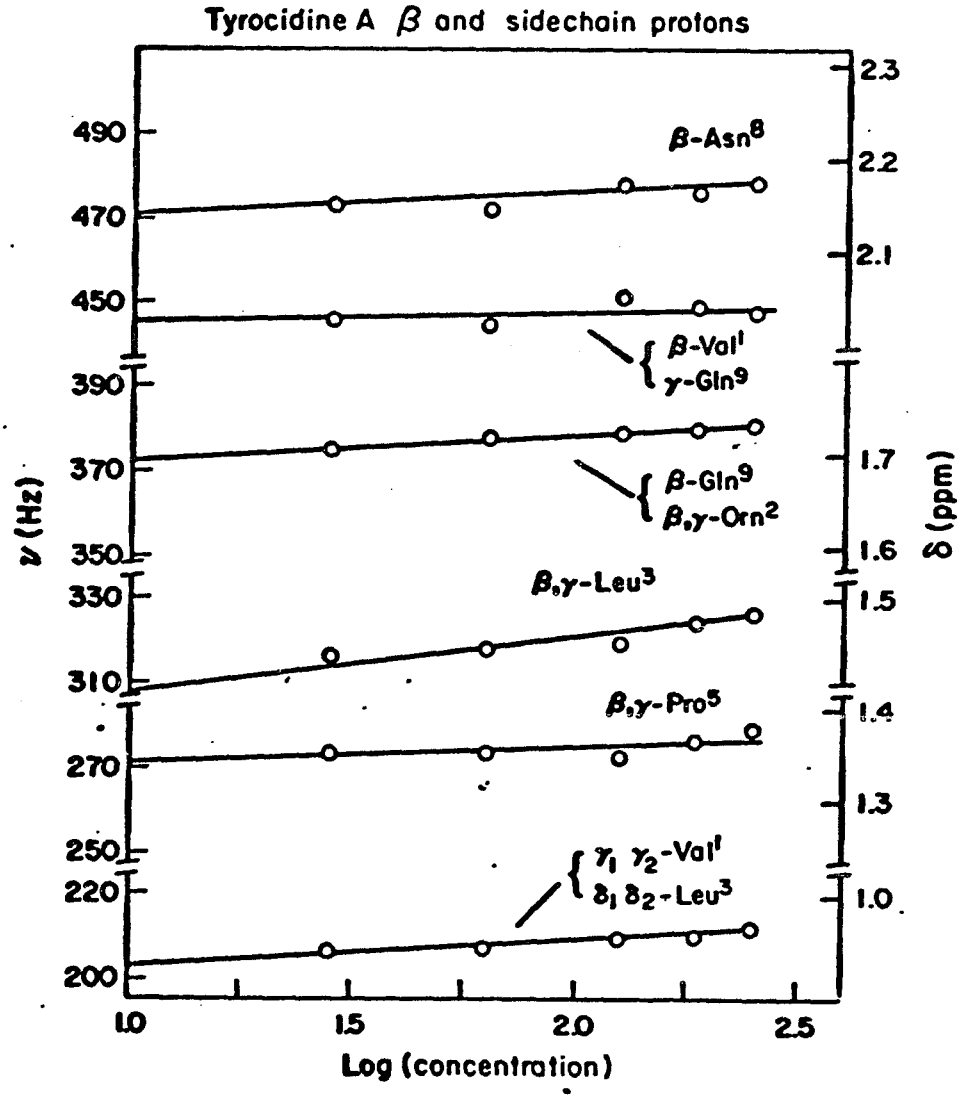

Figure 16

Chemical Shifts of the C^{β} and Side-Chain Protons of Tyrocidine A in $(CD_3)_2SO$ at $20^{\circ} \pm 2^{\circ}C$ as a Function of Concentration (mg/ml).

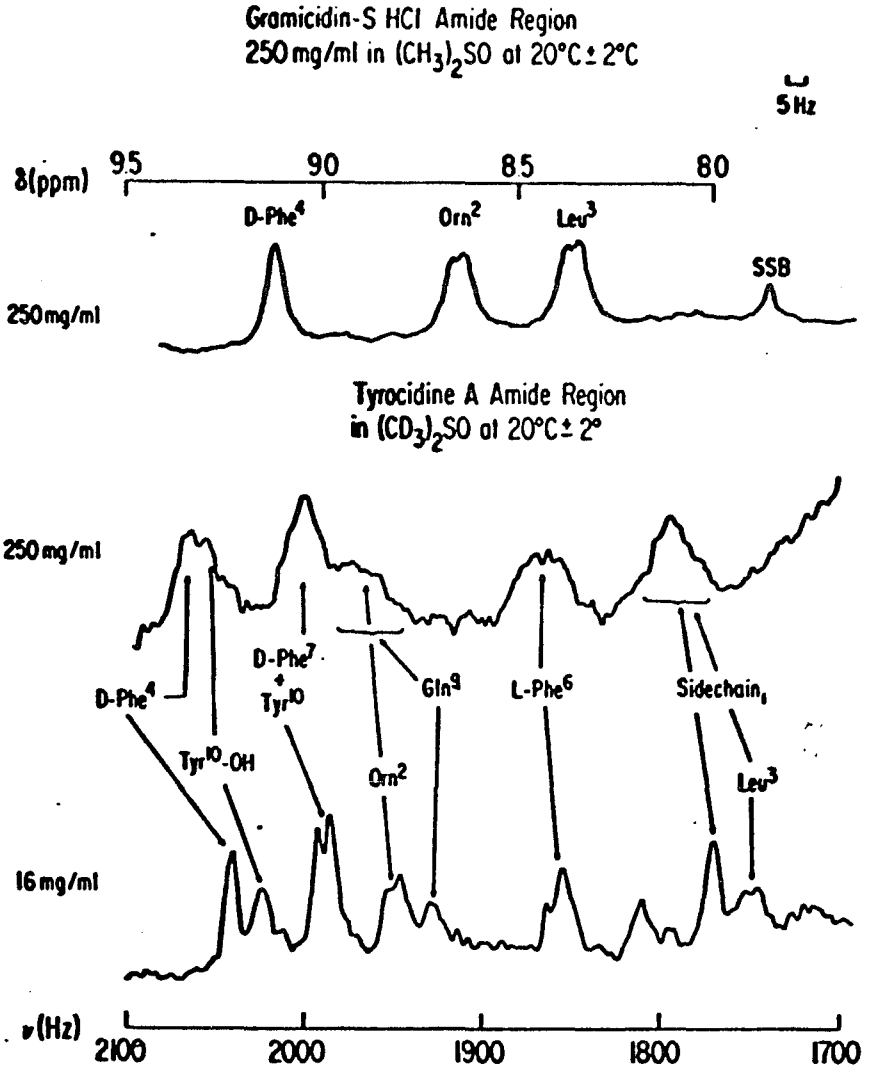

Figure 17

500-Hz Sweep Width Spectra of the Amide Protons of Gramicidin S and Tyrocidine A in $(CD_3)_2SO$ at $20^{\circ} \pm 2^{\circ}C$ for Comparison of Line Widths.

Tyrocidine A spectra at the upper and lower concentrations are shown. Contrast the line widths in the spectrum of 250 mg/m tyrocidine A with those in that of 250 mg/ml gramicidin S.

A possible explanation of this behavior could be rationalized by virtue of the anomalously large exchange rate of this proton in both compounds. As a function of peptide concentration, there is a greater amount of "free" acid which is a concomitant of the lyophylization stage of the preparation of these molecules. Thus, as peptide concentration is increased, the $(CD_3)_2SO$ becomes more "acidified."

Proton exchange rates are very sensitive to changes in acidity, for H^+ can serve as a catalyst for exchange (55). The amide protons of D-Phe^4 in both tyrocidine A and gramicidin S are known to exchange rapidly in $(CD_3)_2SO/D_2O$ mixtures. This rapid exchange is perhaps catalyzed by the H^+ in the contaminating acid. In any event, if there is indeed rapid exchange between H^+ and the proton on the nitrogen of D-Phe^4, then the apparent chemical shift of the amide proton of this residue represents an averaged chemical shift of the two sites. As the $(CD_3)_2SO$ becomes more acidified with an increase in peptide concentration, the observed proton spends a larger fraction of its time in the H^+ pool waiting its turn to replace another proton on the nitrogen of D-Phe^4. Thus, as concentration of peptide is increased, the observed chemical shift of the amide proton would move

downfield towards the chemical shift of the H^+ site (H^+ resonates far downfield because the absence of a surrounding electron causes it to be completely deshielded).

The "acidity" of the $(CD_3)_2SO$ as a function of peptide concentration should also influence the HDX rates of all the amide protons. Thus, higher concentrations of peptide should exhibit enhanced HDX rate constants. Based on this, an HDX study was performed, as previously described, but on a tyrocidine A concentration of 57 mg/ml, approximately a 50 percent increase in peptide concentration above that used in the earlier study. A plot of the rate constants at one concentration versus the corresponding rate constant at the other concentration should yield a monotonic relation if all the protons are being affected by the same non-specific factor. This relationship should be true even if the proton is involved in an intramolecular hydrogen bond.

The data are presented in Table IV and plotted in Figure 18. They are consistent with the above hypothesis. Additionally, the similarity of the behavior of the D-Phe^4 amide proton in both molecules under all conditions studied is presented in Figure 27 and will be discussed below. The virtually identical behavior of this proton in both gramicidin S and tyrocidine A provides very strong

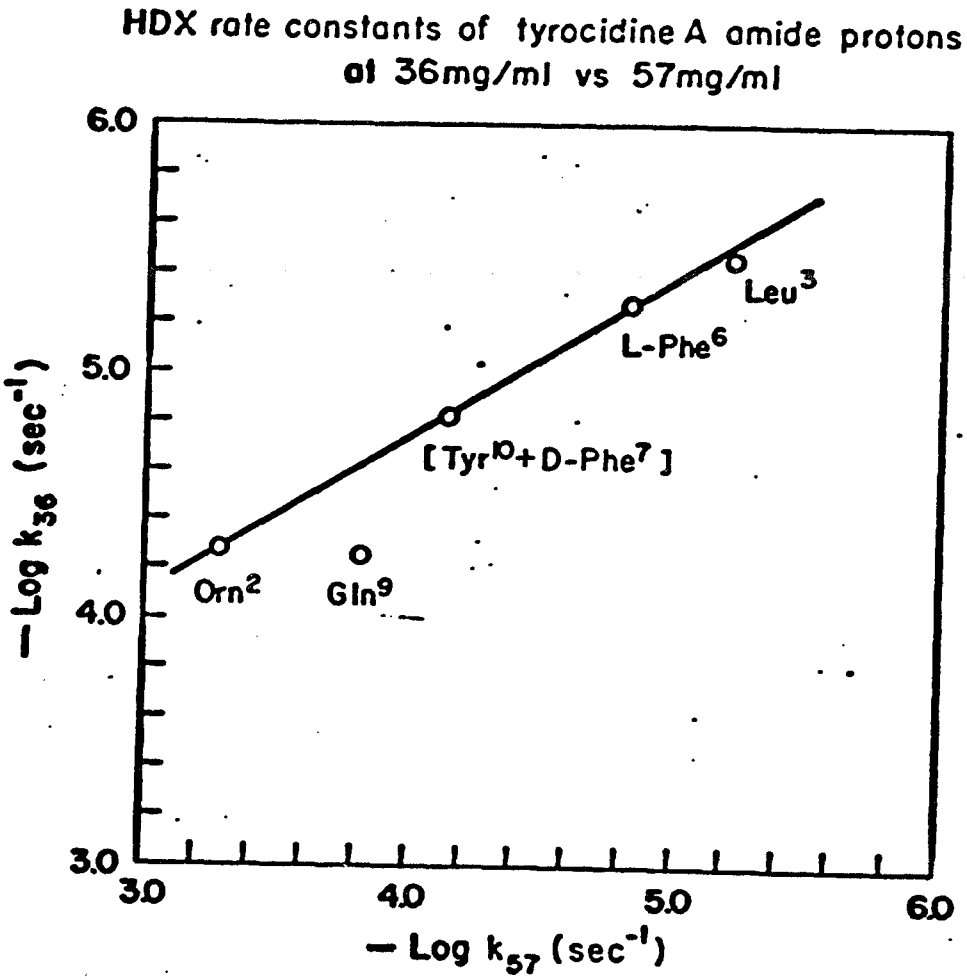

Figure 18

Hydrogen-Deuterium Exchange (HDX) Rate Constants of Tyrocidine A Backbone Amide Protons in $(CD_3)_2SO$ at 20°-25°C at 36 mg/ml vs. 57 mg/ml.

NOTE: The points of this plot were obtained by taking the negative logarithm, base ten, of the calculated rate constant k (Table IV).

Table IV

Concentration Dependence of Hydrogen-Deuterium Exchange (HDX) Rate Constants (k) of Backbone Amide Protons of Tyrocidine A in $(CD_3)_2SO$ at 20-25°C

Residue	$k \times 10^6$ (sec^{-1})	
	36 mg/ml	57 mg/ml
Orn^2	51	520
Leu^3	3.5	6.1
L-Phe^6	5.2	15
D-Phe^7 + Tyr^{10}	15 (avg)	73 (avg)
Gln^9	56	150

supportive evidence that their environments and, therefore, their conformations are the same in both molecules. This similarity strengthens the reasoning for placing the D-Phe^4 residue in tyrocidine A at the first corner position of a β-turn. On this basis, the involvement of Leu^3, Pro^5 and L-Phe^6 in tyrocidine A in a β-turn structure is also enhanced.

Lastly, it may be observed that, on the basis of its lability and solvent-exposed position, the chemical shift behavior of the tyrosyl OH proton is not indicative of aggregation.

The remaining changes in chemical shifts in tyrocidine A, which are concentration-dependent, are not due to exchange processes. This must be true for the C^{α} and side-chain protons since they are not labile. Explanation of the concentration-dependent changes in the chemical shifts of these non-labile protons and those of the remaining amide protons must be based on new juxtapositions of magnetically anisotropic groups which change the effective magnetic field experienced by these protons.

As a first approximation in the attempt to deduce quaternary structure, two assumptions were made:

(1) The larger the chemical shift, the closer the disturbed proton is to the source of the disturbance.

(2) Since small perturbations in the chemical shifts may be caused by phenomenon as yet uncharacterized, but unrelated to aggregation, the chemical shift should have a magnitude greater than 0.045 ppm (10 Hz) over the concentration range studied to be considered significant.

By these criteria, the amide protons of Leu^3, $L\text{-}Phe^6$ and Gln^9 (Figure 13), the C^α proton of Orn^2, the envelope containing the four C^α protons of Val^1, Leu^3, Asn^8 and Tyr^{10}, and Pro^5 (Figure 15) exhibited significant downfield chemical shifts. Inspection of the CPK model for the proposed conformation of tyrocidine A indicated that the amide protons of Leu^3 and $L\text{-}Phe^6$ plus the C^α protons of Orn^2, Leu^3 and Pro^5 are clustered about the left-hand side of the backbone ring when it is viewed as shown in Figure 9. An aromatic side chain, properly oriented in the cavity formed by the Orn^2, Leu^3 and $D\text{-}Phe^9$ residues, could account for these observed shifts.

If the side chain of $L\text{-}Phe^6$ from a second molecule is tilted approximately 20^o with respect to the plane formed by the under surface of its backbone and placed in the cavity of the first molecule, the required shifts can be produced. In addition, the pronounced shift out of the envelope of the resonance of one of the C^α protons

located at 4.5 ppm (1090 Hz), Figure 17, can be attributed to the proximity of the intruding L-Phe^{6} residue from the adjacent molecule in the aggregate to the C^{α} proton of Leu^{3}. This shift is further illustrated in the difference spectra of this region shown in Figure 19.

Juxtaposing the lower surface of the upper molecule with the upper surface of the lower molecule, as above, also aligns the molecules in parallel with respect to their primary sequence. That is, the direction in going from Val^{1} to Tyr^{10}, in what would be the N terminal to C terminal direction in a linear peptide, is the same (counter-clockwise) for both molecules when viewed from what is arbitrarily designated to be the top. Inspection of Figures 13, 15 and 16 shows that the chemical shifts of the proton resonances assigned to Leu^{3} become progressively smaller as their distance from the intruding L-Phe^{6} side chain increases. Hence, the chemical shifts for the protons of Leu^{3}, in order of decreasing magnitude, are those of the amide proton, C^{α} proton and cluster of C^{β} and C^{γ} protons. It can also be seen in Figure 16 that the chemical shift of the C^{β} proton assigned to Val^{1} is virtually independent of concentration. This observation suggests that the placement of the disturbing L-Phe^{6} side chain is correct, since Val^{1} is located on the other side

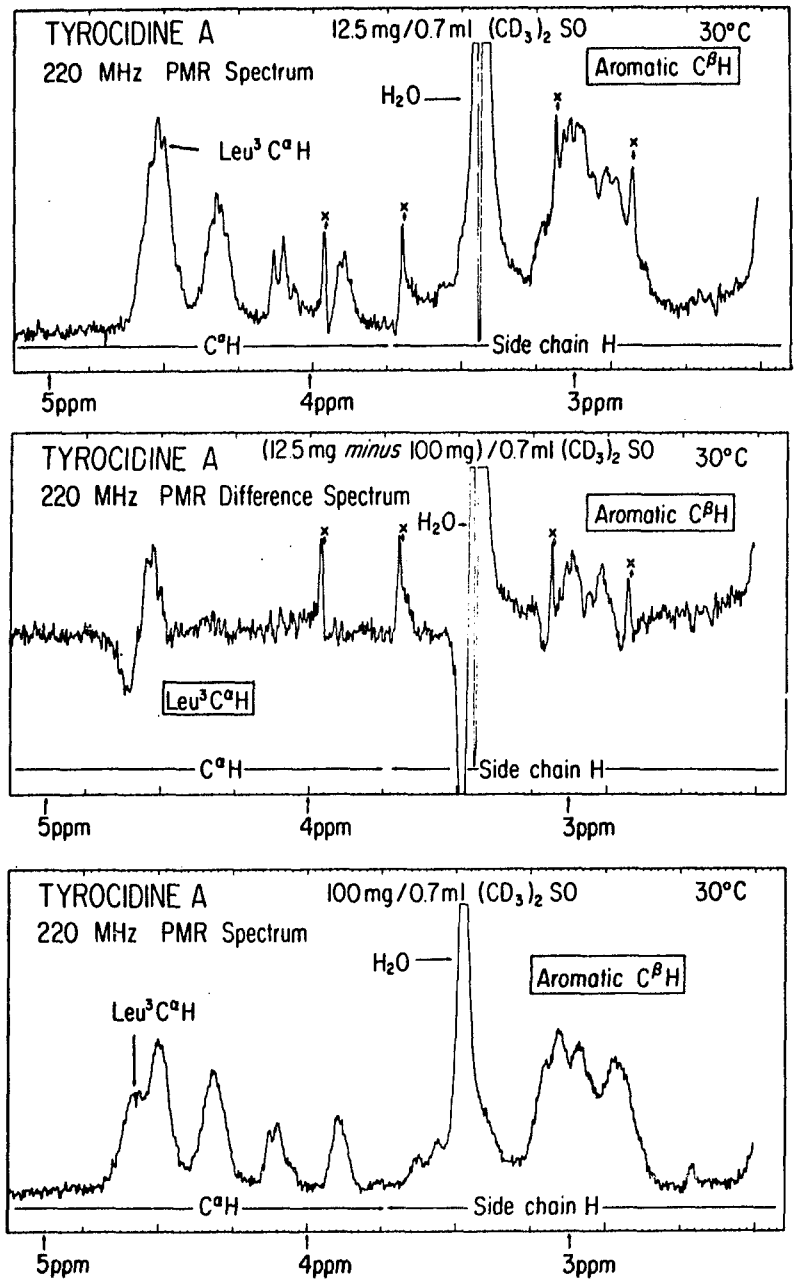

Figure 19

Difference Spectra of the Upfield Portion of the C^{α} Proton Region of Tyrocidine A in $(CD_3)_2SO$ at $28^{\circ} \pm 2^{\circ}C$.

NOTE: The spectra were aligned on the largest peak of the most downfield C^{α} proton envelope (the one assigned as containing the C^{α} protons of Val^1, Leu^3, Asn^8 and Tyr^{10}) located at 4.56 ppm (1000 Hz). This was done to bring out clearly the concentration-dependent C^{α} proton shift.

of the molecule away from this disturbance (i.e., the right-hand side of the molecule when viewed from the top, as shown in Figure 9).

The changes in the chemical shifts of the C^{α} proton and cluster of C^{β} and C^{γ} protons of Pro^{5} can be explained by the same argument used to explain the behavior of the Leu^{3} proton chemical shifts.

By this hypothesized juxtaposition of the two molecules, the chemical shift of the Gln^{9} amide proton is attributed to the carboxamide oxygen of the Asn^{8} residue of the upper molecule. Additionally, the resonance of the Orn^{2} δ-NH_3^+ group of the lower molecule is downfield shifted, the same order of magnitude as the resonances of the Gln^{9} amide proton, by the carbonyl oxygen of the peptide bond of the ornithyl residue of the upper molecule.

Two other aspects of the changes in chemical shifts deserve consideration--viz., their magnitudes and the "linearity" of their excursions over the concentration range studied. Ring current shifts produced by the side chains of aromatic residues can have considerable magnitudes, e.g. 1 ppm (220 Hz) (43). As indicated previously, these shifts are a function of distance and orientation. In the proposed aggregate, however, an additional consideration is required--viz., the superposition of effects

of all of the groups causing anisotropic shifts. Thus, one observes the net effect of these groups on various chemical shifts. For example, in some cases, aggregation may bring more than one anisotropic group in proximity to a particular proton; one group may tend to shield the proton (move its resonance upfield), while the other one may tend to deshield it (move its resonance downfield); only a net effect on the proton will be observed--i.e., the stronger of the two contributing effects will prevail.

The magnitude of the downfield shifts for the conformationally adjacent Leu^3 and L-Phe^6 amide protons (e.g., see Figure 1) can be understood in this way. The L-Phe^6 amide proton will "see" the shielding zone of its own side chain from its lower surface and the deshielding zone of an intruding L-Phe^6 side chain from a second molecule on its upper surface. The resultant, observed shift represents the <u>resultant</u> effective magnetic field as sensed by this proton. The Leu^3 amide proton only "sees" the deshielding zone of the intruding L-Phe^6 side chain. Consequently it is shifted further downfield than the L-Phe^6 amide proton.

The chemical shift behavior of the protons of tyrocidine A clearly indicate that more than one process is occurring. These processes may be related to different aggregate forms, changes in side chain rotomer populations, slight

perturbations of the backbone conformation, different sizes of aggregates formed, and perhaps differential aggregate lifetimes. No attempt has been made at this stage to resolve these possible effects. Instead, the proposed quaternary structure presented is that of the predominant form contributing to the pmr spectra.

In conjunction with the complexity of the aggregation processes indicated by the chemical shift data, a preliminary experiment on proton spin-lattice (longitudinal) relaxation times (T_1) was even more confounding in its difficulty. Initially, it was hoped to obtain an estimate of the rotational correlation times (τ_c) at the various concentrations of tyrocidine A and from them an estimate of molecular size (56). The data obtained for tyrocidine A proved to be intractable to analysis so that they could be correlated with events on the molecular level. It may be stated qualitatively, however, that the behavior exhibited by gramicidin S was a linear function of concentration, while that of tyrocidine A was multiphasic. This indicates that at different concentrations there are differential contributions to the relaxation process, each of which becomes predominant at different concentrations.

Line-width data, which provide information about

spin-spin (transverse) relaxation (T_2) processes, proved more amenable to analysis. Dipole-dipole interaction will cause broadening of the resonance absorption signal. Thus, as groups remain in relatively close contact, each can cross-relax the protons of the other. This exchange of nuclear spins shortens the lifetimes of the spin states of the protons. Therefore, as a consequence of the uncertainty principle, the decrease in the lifetime of a spin state is reflected by a proportional increase in the uncertainty of the energy, i.e., resonance energy. Hence, the signal broadens.

Line-shape analysis for the determination of the line width at half-maximal intensity was performed with a computer program developed by Dr. H. R. Wyssbrod for the Hewlett-Packard HP-65 Fully Programmable Calculator. The data are presented in Figure 20. Spectral analysis could be performed only on those amide protons which did not overlap. The line widths were normalized with respect to their minimal values, which occurred at the lowest concentration.

Examination of Figure 20 shows the striking similarity in behavior of the D-Phe^4 amide proton in both compounds at the lower concentrations. They are probably responding to the same influence with the same magnitude of response

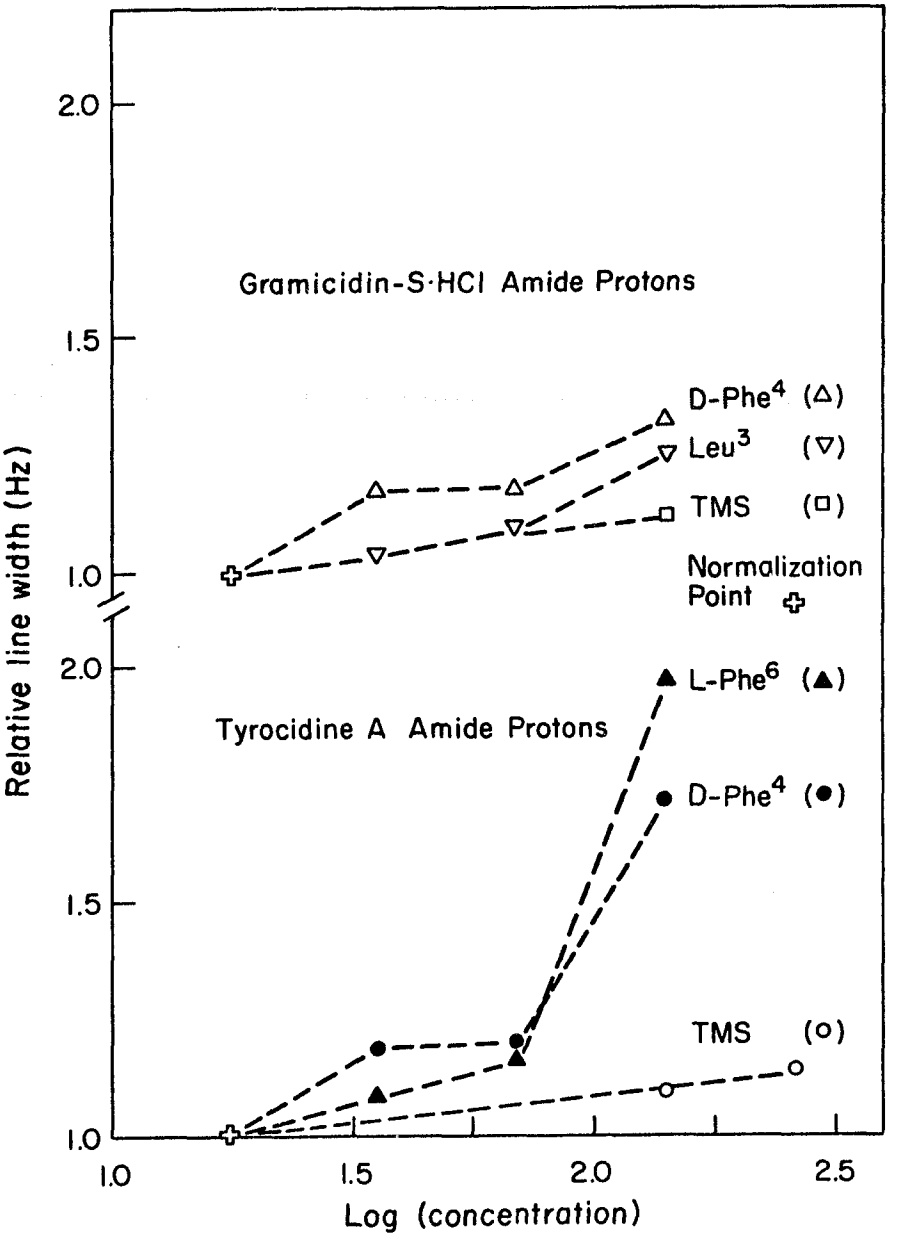

Figure 20

Relative Line Widths of Representative Amide Protons of Gramicidin S and Tyrocidine A in $(CD_3)_2SO$ at $28^o \pm 2^oC$ and $20^o \pm 2^oC$, Respectively, as a Function of Concentration (mg/ml).

at these concentrations. As a function of concentration, there is a dramatic increase in the line width for the representative resonances of the tyrocidine A amide protons but not for those of the gramicidin S amide protons. The line width of TMS (the reference for chemical shift measurements) has been included as a rough estimate of bulk viscosity changes. Thus, the line widths of the representative protons for tyrocidine A nearly doubles, while for gramicidin S the increase is only about 25 percent. The changes observed for tyrocidine A cannot be attributed to bulk viscosity changes as a function of the number of particles in solution, inasmuch as the size and weight of tyrocidine A and gramicidin S molecules are almost equal. Hence, for the above statement to obtain they should both exhibit similar line widths at equivalent concentrations, which is clearly not the case.

In addition, as will be discussed below, the line broadening as a function of concentration persists in tyrocidine A even when the aromatic groups are hydrogenated to form non-aromatic alicyclic groups. This data is thus consistent with enhanced dipolar relaxation caused by spin-spin exchange between at least two peptide molecules (i.e., members of the aggregate). An extreme example of this mechanism and its effect on spectral line width was

shown by Stern et al. for tyrocidine B in D_2O (57).

Figures 21 and 22 illustrate the proposed quaternary structure for the aggregate as deduced from the pmr data. Unfortunately, no independent estimates of aggregate size or weight have been obtained in $(CD_3)_2SO$. The dimer represented by the CPK models in Figures 21 and 22 is only intended to approximate the most probable orientation of the molecules consistent with the nmr data. Thus, one can speculate that, as more molecules are added, the aggregate would form a cylinder. Estimates based on the proportions and pitch of the dimer indicate that about eight monomers could yield closure. This is in good agreement with the ultracentrifugation data of Williams (15) for tyrocidine A aggregates in aqueous solution. The cylindrical octomer would have at one end a hydrophilic cluster of side chains--viz., those of Asn^8, Gln^9, Tyr^{10}; the hydrophobic side chain of Val^1 would be buried between the molecules and thus not be solvent exposed. The side chains of Orn^2 would be wrapped around the middle of the outer surface of the cylinder. The D-Phe^4-Pro^5 end of the cylinder would be the hydrophobic end. The L-Phe^6 side chain would be sandwiched between molecules and therefore be solvent shielded.

This proposed model of an octomer is in good agreement

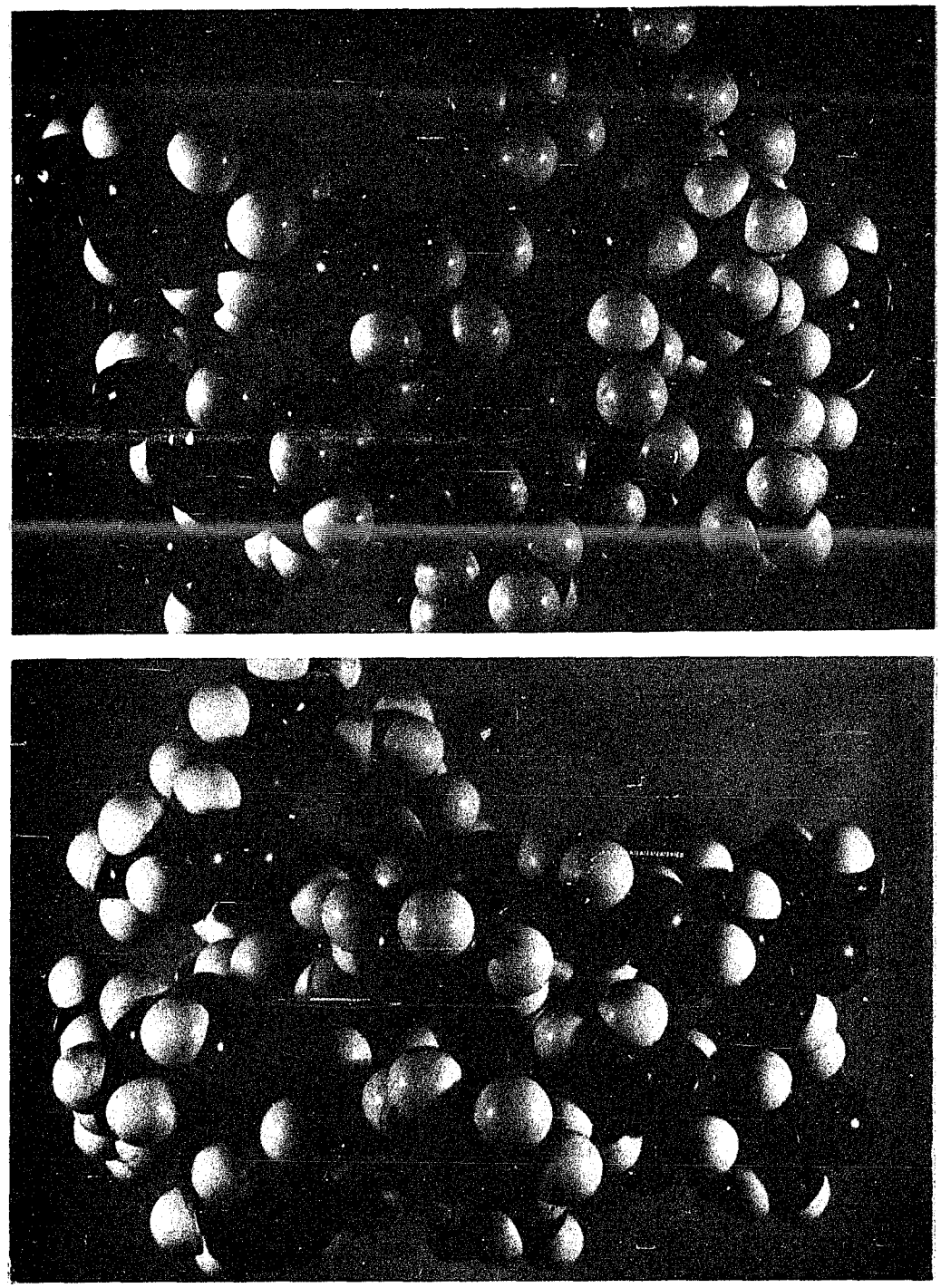

Figure 21

CPK Model of the Proposed Mode of Aggregation for Tyrocidine A in $(CD_3)_2SO$ Viewed Edgewise with Respect to the Backbone Ring.

For clarity only two molecules are shown:
- Upper photograph residue sequence (from left to right): $Tyr^{10} \rightarrow Val^{1} \rightarrow Orn^{2} \rightarrow Leu^{3} \rightarrow D\text{-}Phe^{4}$.
- Lower photograph residue sequence (from left to right): $Pro^{5} \rightarrow L\text{-}Phe^{6} \rightarrow D\text{-}Phe^{7} \rightarrow Asn^{8} \rightarrow Gln^{9}$.

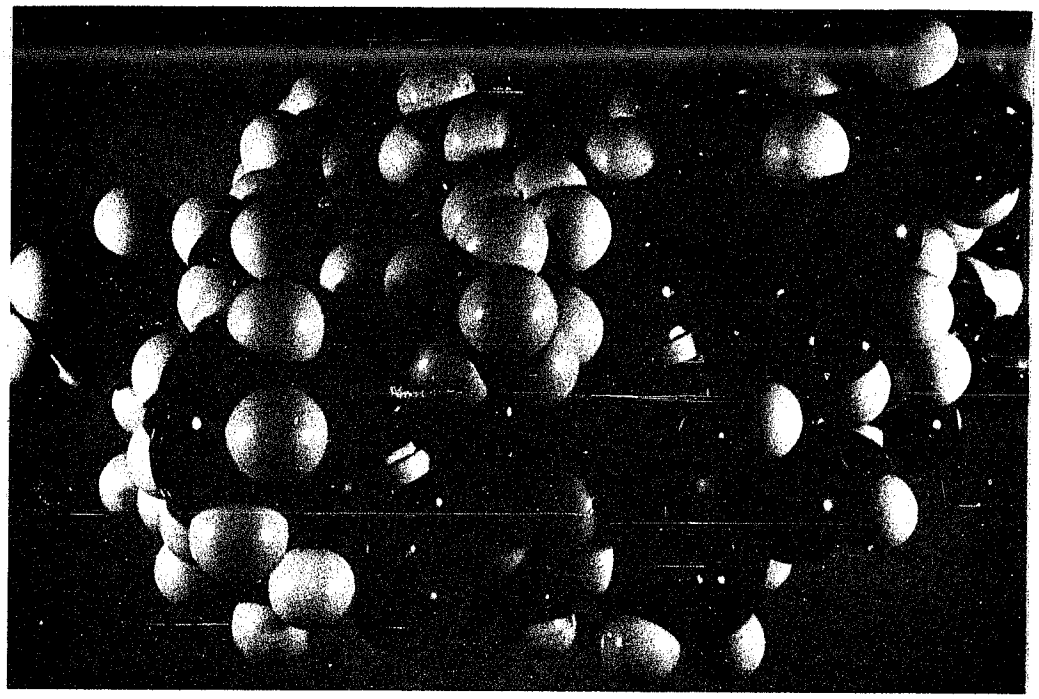

Figure 22

CPK Model of the Proposed Mode of Aggregation for Tyrocidine A in $(CD_3)_2SO$ Viewed from the Upper Surface.

For clarity only two molecules are shown:
Orientation: D-Phe^4 → Pro^5 β-turn on the left;
Gln^9 → Tyr^{10} β-turn on the right.

with results obtained by Laiken (16), who studied the aggregation of tyrocidine B in aqueous solution (this peptide differs from tyrocidine A by the substitution of a tryptophyl residue for a phenylalanyl residue at position 6). Laiken observed a blue shift in the fluorescence maximum of the Trp^6 indole ring as a function of peptide concentration. A blue-shifted fluorescence maximum is an indication of an increasingly apolar environment (58, 59). Thus, sandwiching the side chain of residue 6 between the molecules in the aggregate away from the solvent is compatible with the fluorescence data.

In the proposed model of the octomer, the D-Phe^7 side chains would be stacked one above another and be "tucked" against the peptide backbone. This arrangement would make them relatively inaccessible to solvent.

It is conceivable, based on the proposed cylindrical octomer structure, that the cylinders could themselves interact to produce larger aggregates by associating their "hydrophobic" ends away from the solvent. Indeed, Williams (15) has suggested that a 24-mer can be formed in aqueous solution. Laiken (16) has obtained electron micrographs of a fibrillar structure produced from "super" aggregates of tyrocidine B in aqueous solution. It is easy to see how the hydrophobic D-Phe^4-Pro^5 ends of

octomers could join to form a hexadecamer (16-mer), but it is not readily apparent how three octomers could join to form a 24-mer nor how many octomers could join to form a large fibrillar structure. Perhaps the fibrillar structure could be obtained by slightly increasing the pitch of the aggregate so that it forms a helix upon addition of molecules without attaining closure, but at this stage this hypothesis is just speculation.

Based on the proposed quaternary structure, predictions about the behavior of the chemical shifts and the line-width parameters can be made. Since most of the amide proton shifts are a result of the ring current anisotropy of the aromatic side chain of L-Phe^6, hydrogenation of tyrocidine A should eliminate them. After hydrogenation, the only shifts in the amide proton region that should be concentration-dependent in the tyrocidine A (reduced) are those of Gln^9 and the Orn^2 δ-NH_3^+ group, since these are produced by carbonyl oxygens, and the shift of the D-Phe^4 amide proton by the previous argument--viz., concomitant acidification of the solvent. In addition, as a function of concentration, tyrocidine A (reduced) but not gramicidin S (reduced) should exhibit line broadening. Lastly, hydrogenation of both gramicidin S and tyrocidine A, by eliminating

the ring current shifts of all aromatic residues, should provide data for assessing the similarities of the backbone conformation between gramicidin S and tyrocidine A by inspection of the chemical shifts of the C^{α} protons.

Tyrocidine A and gramicidin S were hydrogenated using the procedure of Keil et al. (60) modified by the substitution of acetic acid for 0.1 M HCl. The concentration studies were repeated under the conditions and by the techniques discussed previously.

Figure 23 shows the 2500-Hz sweep width spectra of gramicidin S and gramicidin S (reduced). Most striking is the complete absence of the signal due to the ten protons of the aromatic rings of the two D-Phe^4 residues, thereby revealing the Val^1 amide proton in the reduced compound. Upon hydrogenation, the two D-phenylalanyl residues are converted into two D-cyclohexylalanyl (D-CXA) residues. Since there are no π electrons in the side chain of CXA, the 22 protons in the two cyclohexyl rings are more shielded than the ten protons in the two aromatic rings and come to resonance upfield in the aliphatic side-chain proton region of the spectrum--i.e., upon hydrogenation of gramicidin S, the ten aromatic protons, resonating at 7.27 ppm (1600 Hz), are converted

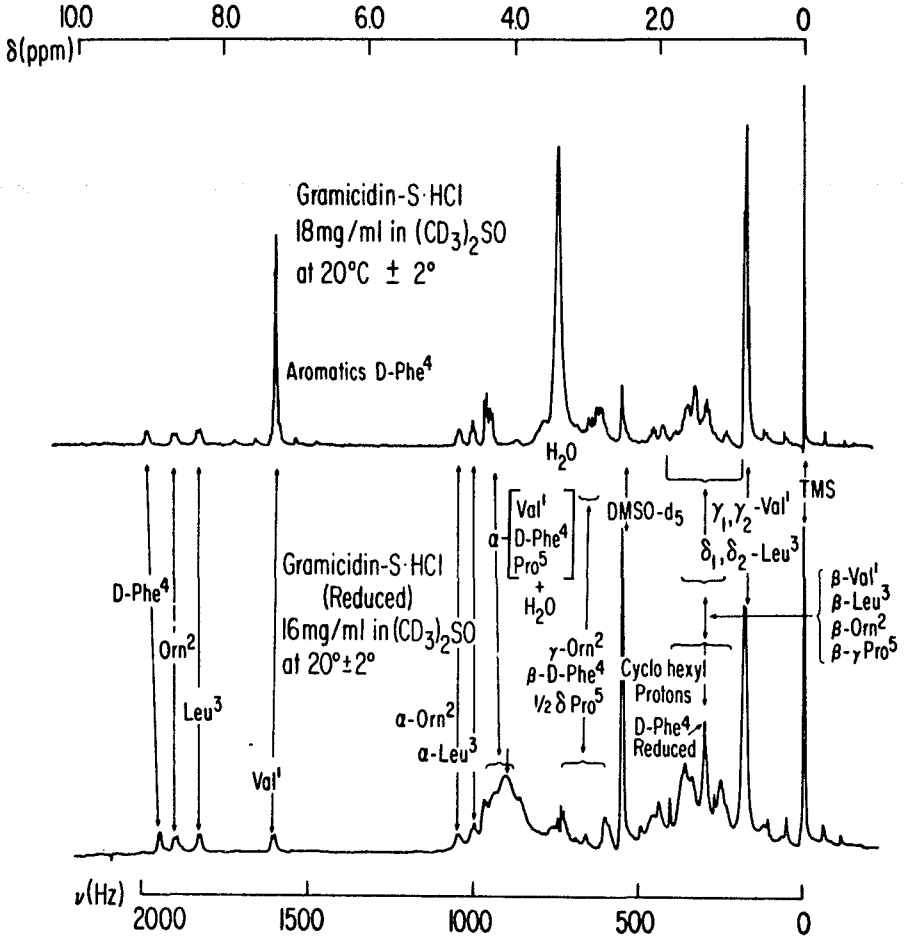

Figure 23

2500-Hz Sweep Width Spectra of Gramicidin S and Gramicidin S (reduced) in $(CD_3)_2SO$ at $20^o \pm 2^oC$.

NOTE: In gramicidin S (reduced) D-Phe^4 becomes D-cyclohexylalanyl^4.

into 22 aliphatic protons resonating in the normal side-chain proton region.

The chemical shifts of the amide protons are relatively unaltered between the reduced and aromatic compounds, with the exception of the D-Phe^4 amide proton. In this context, it is interesting to note that reduction of the D-Phe^4 side chain leads to an observed upfield shift of its amide proton of only 0.23 ppm (50 Hz), the same order of magnitude as that produced by the L-Phe^6 residue in the aggregation studies of tyrocidine A. Lastly, the C^{α} protons have virtually identical chemical shifts in both the reduced and aromatic compounds.

Figure 24 presents the 2500-Hz sweep width spectra of tyrocidine A and tyrocidine A (reduced). The amide protons in the reduced compounds were assigned on the basis of their temperature dependences at 20°C and 30°C, their coupling constants, and their relative chemical shifts. For the concentration studies reported below, the critical assignment is that of the Gln^9 amide proton. Fortunately, Gln^9 has a small amide-C^{α} proton coupling constant (2.7 Hz); thus, the resonance of the amide proton of Gln^9 can be distinguished from the majority of the resonances of the other amide protons on this basis. The only other amide proton with a small coupling

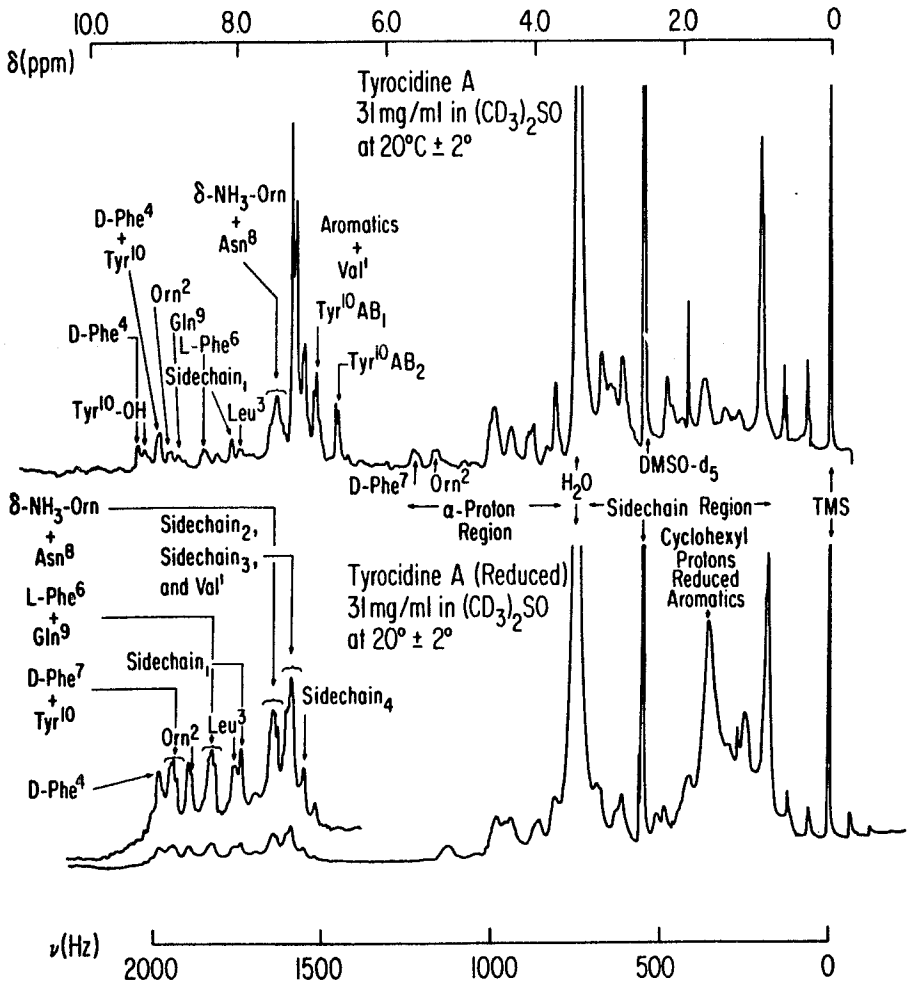

Figure 24

2500-Hz Sweep Width Spectra of Tyrocidine A and Tyrocidine A (reduced) in $(CD_3)_2SO$ at $20^o \pm 2^oC$.

NOTE: Phenylalanyl residues become cyclohexylalanyl residues in tyrocidine A (reduced). Assignments in tyrocidine A (reduced) are only tentative.

constant is that of D-Phe^4 (2.4 Hz), but its chemical shift is at the most downfield position of the amide proton region. Examination of Figure 24 shows the absence of the 19 downfield aromatic protons (15 from phenylalanyl and four from tyrosyl residues) and their replacement, upfield, by 44 cyclohexyl protons as a consequence of hydrogenation.

Inspection of the C^{α} proton region reveals considerable changes in going from the non-reduced to the reduced tyrocidine A. The C^{α} protons assigned to Orn^2 and D-Phe^7 in the non-reduced peptide execute 0.20 ppm (45 Hz) and 0.50 ppm (110 Hz) upfield shifts, respectively, coming to resonance at 5.1 ppm (1125 Hz)--i.e., they become magnetically equivalent. The large upfield shift of the D-Phe^7 C^{α} proton can be rationalized on the basis of its orientation. It comes within the deshielding zones of its own as well as the L-Phe^6 side chains in non-reduced tyrocidine A.

The upfield C^{α} protons assigned to Val^1, Leu^3, D-Phe^4, L-Phe^6, Asn^8 and Tyr^{10} form one large envelope centered around 4.3 ppm (950 Hz). Thus, as a result of the hydrogenation removing the ring-current anisotropy, the chemical environments and, hence, the magnetic environments of these protons become more equivalent.

Comparison of the C^{α} proton regions of reduced gramicidin S and reduced tyrocidine A led to some interesting conclusions. Firstly, the chemical shifts of the Orn^{2} and D-CXA^{7} C^{α} protons in reduced tyrocidine A are identical. The most likely hypothesis is that the magnetic anisotropy of the D-Phe^{7} aromatic side chain contributes to the anomalously downfield position of its own C^{α} proton in the non-reduced analogue. Upon hydrogenation, the only groups capable of producing large magnetic anisotropic shifts are the carbonyl oxygens of the side chains (in tyrocidine A) and the peptide linkages (in both gramicidin S and tyrocidine A).

The most downfield C^{α} proton in gramicidin S is that of Orn^{2}. This anomalous chemical shift has never been explained (19, 61). Comparison of the most downfield C^{α} protons in reduced tyrocidine A with those in reduced gramicidin S shows that this anomalous effect is more pronounced in tyrocidine A. If the secondary structure (backbone conformation) of both molecules were identical, one would expect that, upon removal of the ring-current shifts by hydrogenation, the C^{α} protons should resonate at approximately the same magnetic field strength. The resonances of the C^{α} protons of Orn^{2} and D-CXA^{7} are 0.34 ppm (75 Hz) more downfield than

their homologous position in gramicidin S.

This difference in chemical shift probably indicates that there are differences in the backbone structure of gramicidin S and tyrocidine A. In order to characterize precisely these differences, one must calculate the net effective magnetic field produced by the backbone peptide linkages and their juxtapositions. From this calculation one may possibly be able to orient the C^{α} protons to produce the required shifts. If this approach proves successful, one should be able to obtain information about the dihedral angle ψ. Such a project would be an enormous undertaking and will not be given further consideration here.

The chemical shift behavior of the amide protons of reduced gramicidin S as a function of concentration is presented in Figure 25. The amide proton of $D\text{-}CXA^4$ behaves as it did in previous studies.

The chemical shift behavior of the amide protons of reduced tyrocidine A is presented in Figure 26. Comparison of their behavior here with their behavior in the non-reduced analogue (Figure 13) and with reduced gramicidin S is as predicted. The only shifts manifested are those of the $D\text{-}CXA^4$ amide proton, the Gln^9 amide proton and the Orn^2 $\delta\text{-}NH_3^+$ group. There are no ring-current shifts.

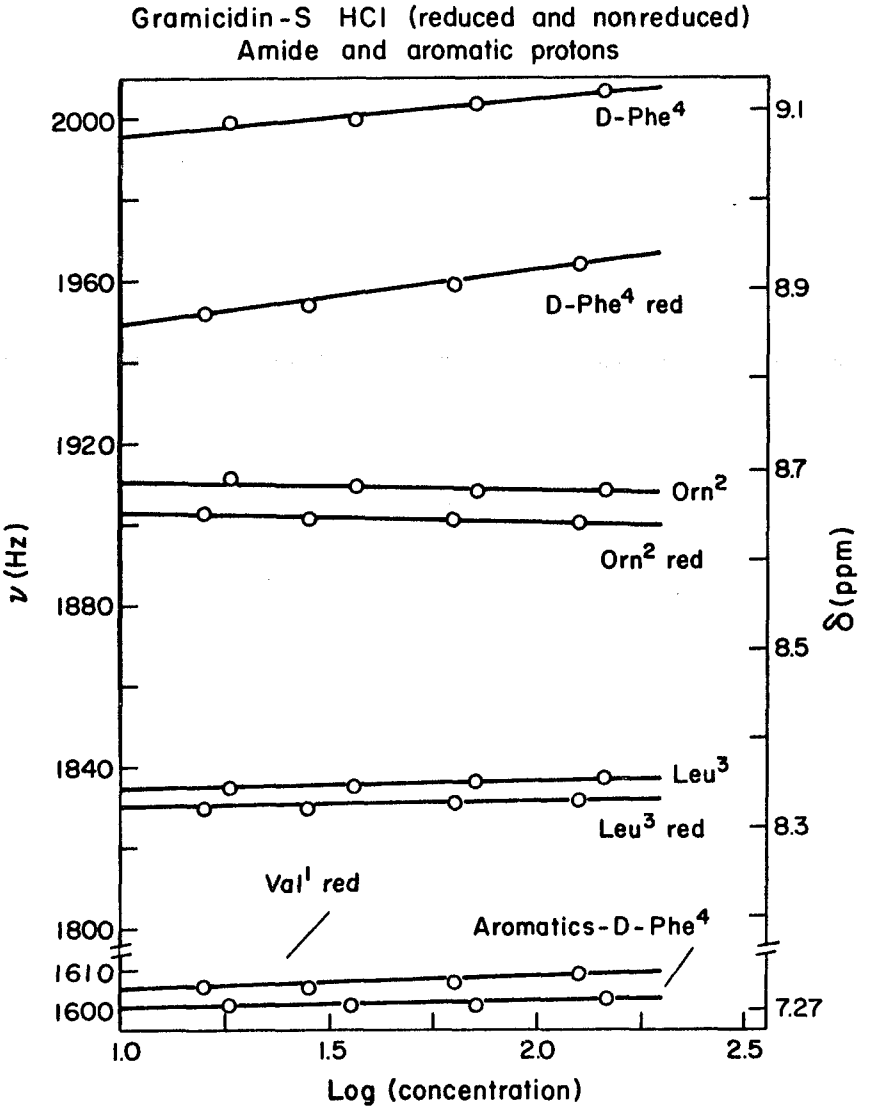

Figure 25

Chemical Shifts of the Amide Protons of Gramicidin S and Gramicidin S (reduced) in $(CD_3)_2SO$ at 20 ± 2°C as a Function of Concentration (mg/ml).

NOTE: D-Phe^4 becomes D-cyclohexylalanyl^4 in gramicidin S (reduced).

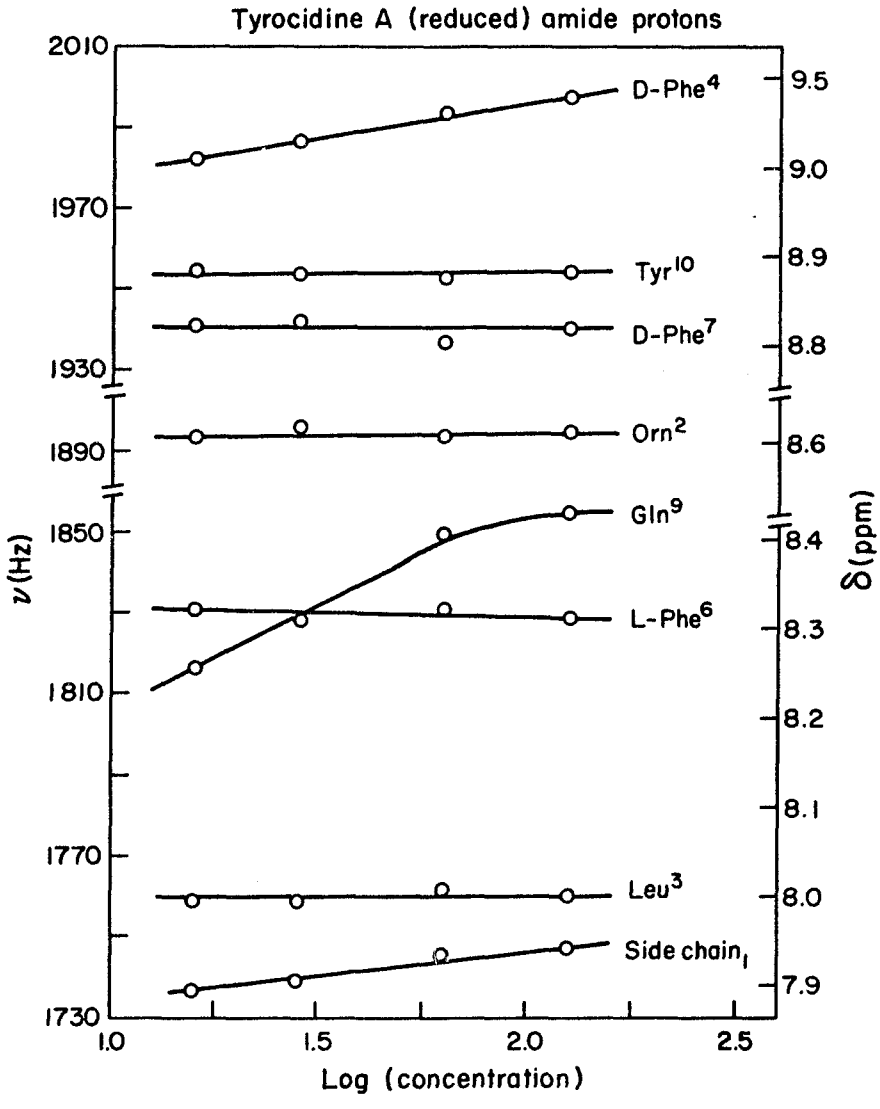

Figure 26

Chemical Shifts of the Amide Protons of Tyrocidine A (reduced) in $(CD_3)_2SO$ at $20^o \pm 2^oC$.

NOTE: The phenylalanyl residues become cyclohexylalanyl residues in tyrocidine A (reduced).
The chemical shift of the ornithyl δ-NH_3^+ is not shown.

The chemical shift behavior of the D-Phe^4 amide proton under all conditions studied, for both gramicidin S and tyrocidine A, is presented in Figure 27. Their behavior is virtually identical under all circumstances and is a reflection of their conformational similarity and not, therefore, an indication of aggregation.

Figures 28 and 29 present the amide region of the reduced compounds gramicidin S and tyrocidine A for comparison of their line widths. As can be seen in Figure 28, there is very little change in the line widths at the extreme concentrations of reduced gramicidin S. In contrast, the line-width changes in reduced tyrocidine A are of the same order of magnitude as observed previously at the corresponding concentrations.

These experiments provide data which are consistent with the proposed quaternary structure of the tyrocidine A aggregate. Additionally, substitution of cyclohexyl groups for phenyl groups on the CPK model did not produce any observable changes in juxtapositions for the proposed structure of the aggregate. Lastly, since the chemical shifts of the amide protons of Leu^3, L-Phe^6, Orn^2, D-Phe^7 and Tyr^{10} (Figure 26) do not change in tyrocidine A (reduced) as the aggregate forms--i.e., they are independent of concentration--they are not

Chemical Shift of D-Phe^4 Amide Proton (Reduced & Aromatic)
Gramicidin-S·HCl & Tyrocidine A at Equivalent Concentrations

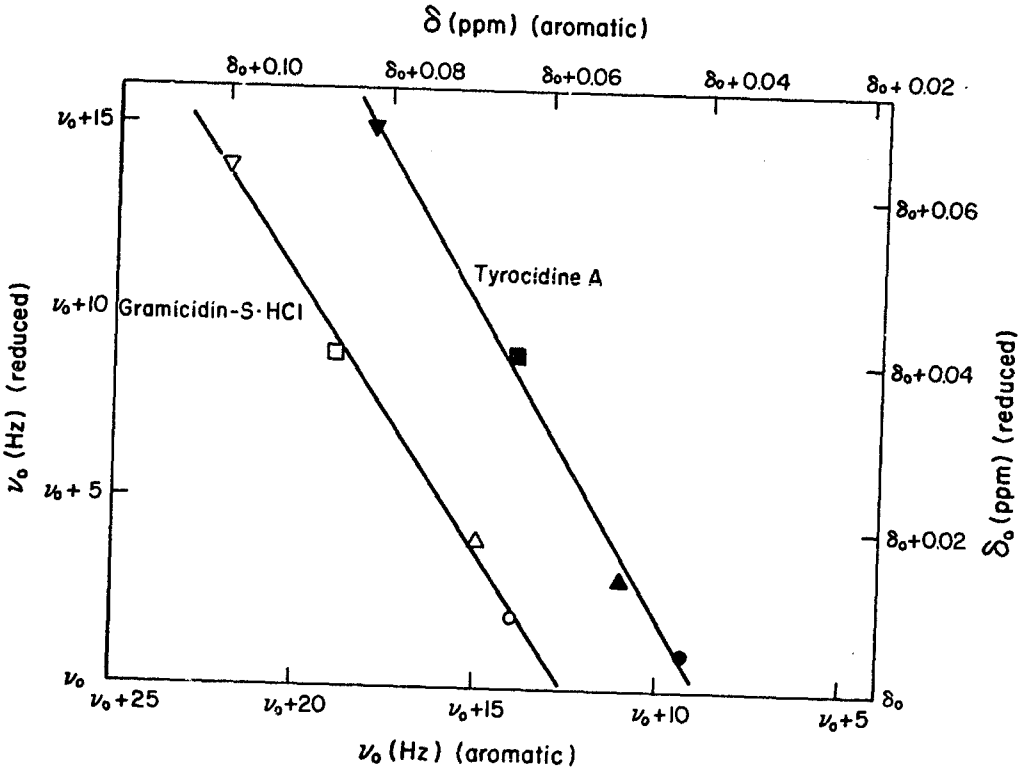

Figure 27

Chemical Shift Behavior of the Amide Proton of Residue 4 in both Gramicidin S and Tyrocidine A for both the Aromatic and Reduced Analogues.

NOTE: The chemical shift scales-- ν (Hz) and δ (ppm)-- are arbitrarily defined so that the excursions of the chemical shifts for both protons can be represented on the same axes. The concentrations correspond approximately to the following values for both molecules:

▽ = 143 mg/ml
□ = 73 mg/ml
△ = 36 mg/ml
○ = 18 mg/ml

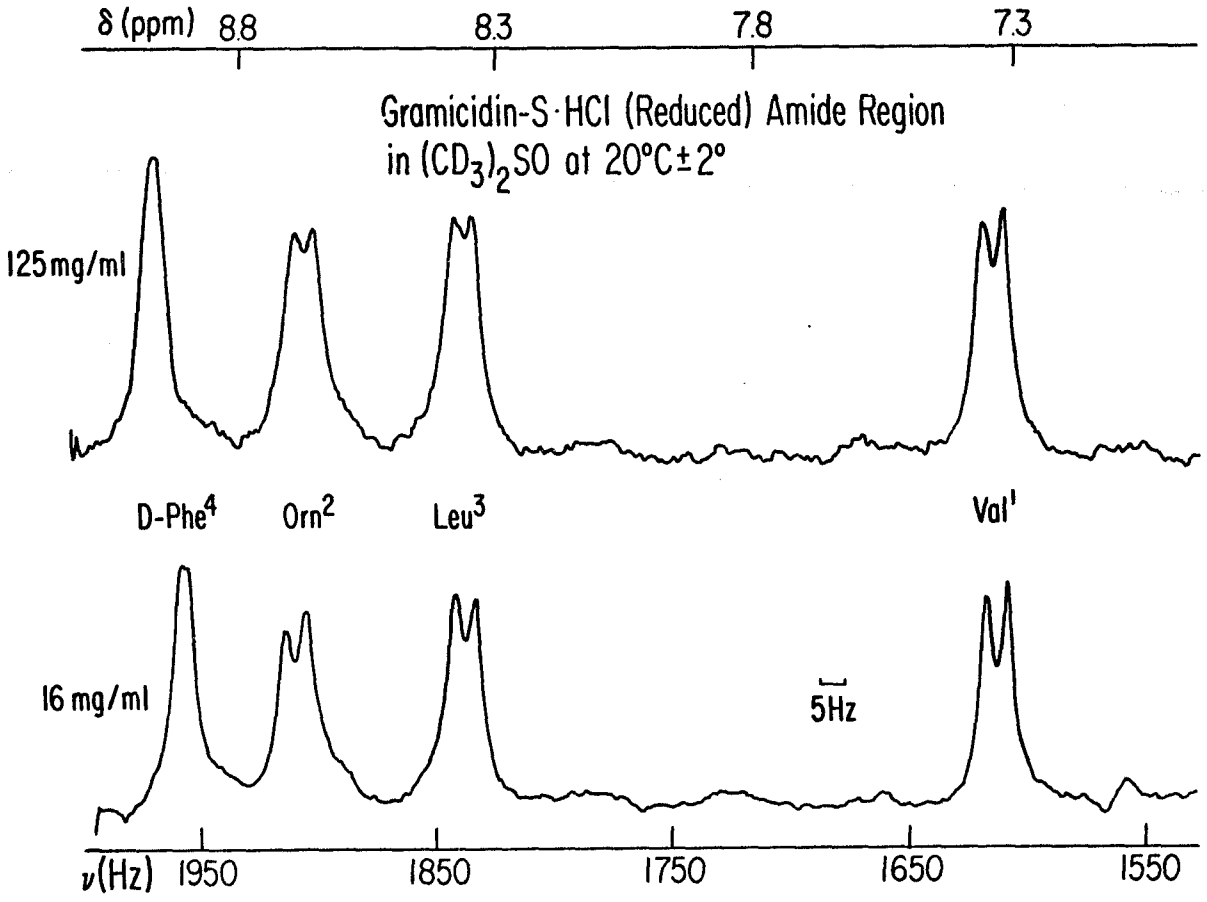

Figure 28

500-Hz Sweep Width Spectra of the Amide Protons of Gramicidin S (reduced) in $(CD_3)_2SO$ at 20° ± 2°C at the Upper and Lower Concentrations for Comparison of Line Widths.

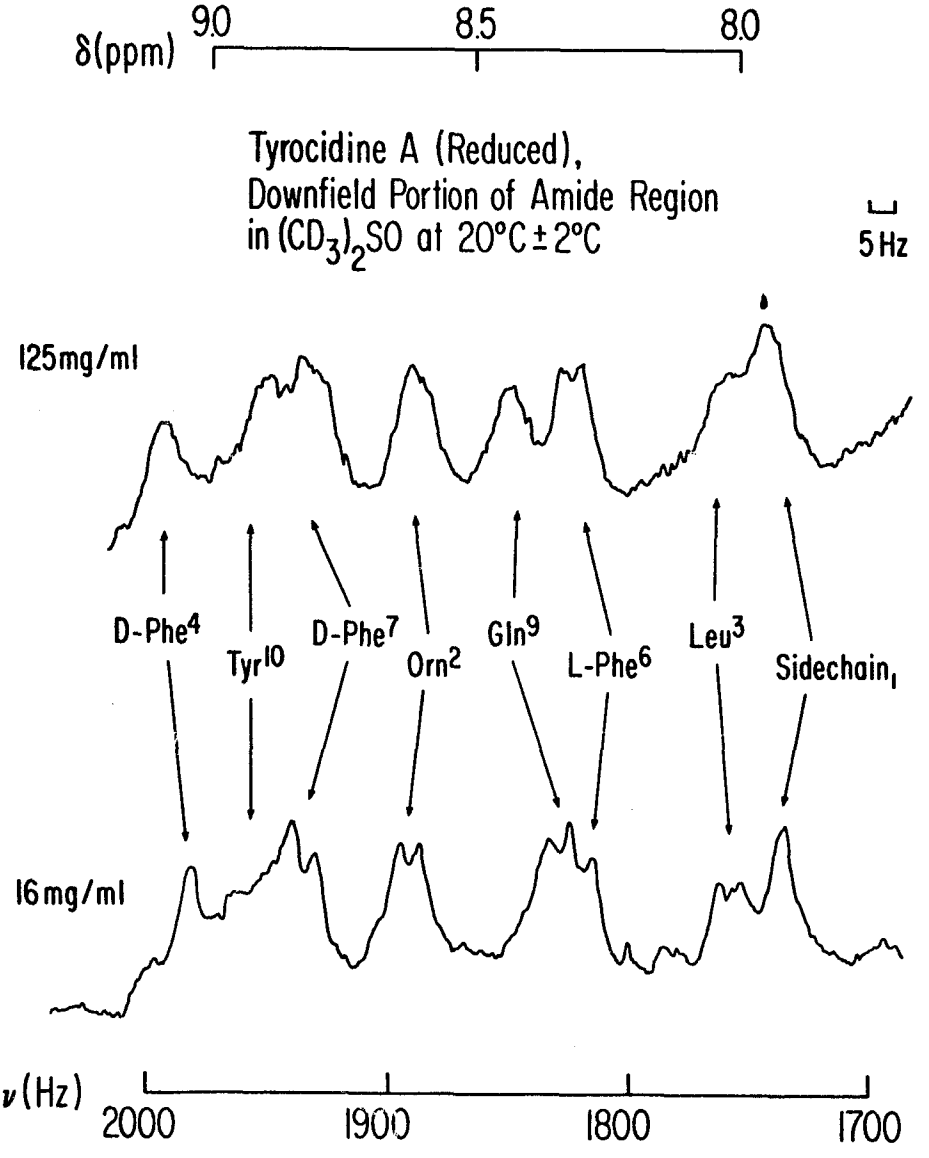

Figure 29

300-Hz Sweep Width Spectra of the Amide Protons of Tyrocidine A (reduced) in $(CD_3)_2SO$ at $20^o \pm 2^oC$ at the Upper and Lower Concentrations for Comparison of Line Widths.

NOTE: The resonance of the ornithyl δ-NH_3^+ group has not been included in the spectra. Its downfield trailing edge may be observed in the right-hand end of the upper spectrum.

involved in stabilizing the aggregate by forming inter-molecular hydrogen bonds. If they were so involved, one would expect differences in the chemical environments between intra- and intermolecular hydrogen bonds and, hence, differences in the chemical shift characteristic of these two environments.

In conclusion, the studies undertaken here indicate that there is considerable complexity in the aggregation of even "model" peptides. This complexity may be a reflection of the scarcity of knowledge regarding these non-covalent interactions or, perhaps, the large number of factors and conditions which must obtain so that these interactions may occur. In either case, the goal of the prediction of higher-ordered structures from primary structure will not be achieved in the near future.

The factors and conditions for the aggregation of tyrocidine A can be probed further with the availability of a workable synthesis for this molecule. Amino acid replacements can, in future studies, prove fruitful in analyzing conformational contributions to the attainment of quaternary structure.

BIBLIOGRAPHY

1. Crick, F.H.C., J. Mol. Biol. 19:548, 1966.

2. Linderstrøm-Lang, K., "Proteins and Enzymes, Lane Memorial Lectures," p. 54, Stanford University Press, Stanford, 1952.

3. Kendrew, J.C., Klyne, W., Lifson, S., Miyazawa, T., Némethy, G., Phillips, D.C., Ramachandran, G.N., and Scheraga, H.A., Biochemistry 9:3471, 1970.

4. Scheraga, H.A., "Protein Structure," Academic Press, New York, 1961.

5. Ramachandran, G.N., Ed., "Conformation of Biopolymers," Vols. 1 and 2, Academic Press, New York, 1967.

6. Flory, P.J., "Statistical Mechanics of Chain Molecules," Wiley (Interscience), New York, 1969.

7. Wyssbrod, H.R., and Gibbons, W.A., "Survey of Progress in Chemistry," Vol. 6., Scott, A.F., Ed., p. 209, Academic Press, New York, 1973.

8. Laland, S., and Zimmer, T., Essays Biochem. 9:31, 1973.

9. Lipmann, F., Acct. Chem. Res. 6:361, 1973.

10. Lipmann, F., Science 173:875, 1975.

11. Sarkar, N., and Paulus, H., Nature New Biol. 239:228, 1972.

12. Schazschneider, B., Ristow, H., and Kleinkauf, H., Nature 249:757, 1974.

13. Ruttenberg, M.A., Doctoral Dissertation, The Rockefeller University, 1965.

14. Ruttenberg, M.A., King, T.P., and Craig, L.C., Biochemistry 5:2857, 1966.

15. Williams, R.C., Jr., Doctoral Dissertation, The Rockefeller University, 1967.

16. Laiken, S.L., Doctoral Dissertation, The Rockefeller University, 1970.

17. Epstein, C.J., Goldberger, R.F., and Anfinsen, C.B., Cold Spring Harbor Symp. Quant. Biol. 28:439, 1963.

18. Kauzmann, W., Advan. Prot. Chem. 14:1, 1959.

19. Stern, A., Gibbons, W.A., and Craig, L.C., Proc. Natl. Acad. Sci. 61:734, 1968.

20. Huggins, M.L., Chem. Rev. 32:195, 1943.

21. Schmidt, G.M., Hodgkin, D.C., and Oughton, B.M., Biochem. J. 65:744, 1957.

22. Hodgkin, D.C., and Oughton, B.M., Biochem. J. 65:752, 1957.

23. Liguori, A.M., De Santis, P., Kovacs, A.L., and Mazzarella, L., Nature 211:1039, 1966.

24. Venkatachalam, C.M., Biopolymers 6:1425, 1968.

25. Chandrasekaran, R., Lakshminayan, A.V., Pandya, U.V., and Ramachandran, G.N., Biochim. Biophys. Acta 303:14, 1973.

26. Beyer, C.F., Gibbons, W.A., Craig, L.C., and Longworth, J.W., J. Biol. Chem. 249:3204, 1974.

27. Laszlo, P., Progr. NMR Spectroscopy 3:231, 1967.

28. Ivanov, V.T., Laine, I.A., Abdulaev, N.D., Senyavina, L.B., Popov, E.M., Ovchinnikov, Y.A., and Shemyakin, M.M., Biochem. Biophys. Res. Commun. 34:803, 1969.

29. Llinás, M., Klein, M.P., and Neilands, J.B., J. Mol. Biol. 52:399, 1970.

30. Llinás, M., Klein, M.P., and Neilands, J.B., Int. J. Peptide Protein Res. 4:157, 1972.

31. Llinás, M., Klein, M.P., and Neilands, J.B., J. Mol. Biol. 68:265, 1972.

32. Battersby, A.R., and Craig, L.C., J. Amer. Chem. Soc. 74:4019, 1952.

33. Ruttenberg, M.A., King, T.P., and Craig, L.C., Biochemistry 4:11, 1965.

34. Gibbons, W.A., Beyer, C.F., Dadok, J., Sprecher, R.F., and Wyssbrod, H.R., Biochemistry 14:420, 1975.

35. Karplus, M., J. Chem. Phys. 30:11, 1959.

36. Karplus, M., J. Amer. Chem. Soc. 85:2870, 1963.

37. Bystrov, V.F., Ivanov, V.T., Portnova, S.L., Balashova, T.A., and Ovchinnikov, Y.A., Tetrahedon 29:873, 1973.

38. Bystrov, V.F., Advan. Magn. Resonance, in press.

39. Pitner, T.P., and Urry, D.W., J. Amer. Chem. Soc. 95:1399, 1972.

40. La Mar, G.N., Horrocks, W.D., and Holm, R.H., Jr., Eds., "NMR of Paramagnetic Molecules; Principles and Applications," Academic Press, New York, 1973.

41. Schneider, W.G., Bernstein, H.J., and Pople, J.A., J. Chem. Phys. 28:601, 1958.

42. Kopple, J.D., Ohnishi, M., and Go, A., Biochemistry 8:4087, 1969.

43. Bovey, F.A., Brewster, A.I., Patel, D.J., Tonelli, A.E., and Torchia, D.A., Acct. Chem. Res. 5:193, 1972.

44. Urry, D.W., and Ohnishi, M., in "Spectroscopic Approaches to Biomolecular Conformation," Urry, D.W., Ed., p. 263, American Medical Association, Chicago, 1970.

45. Gibbons, W.A., Némethy, G., Stern, A., and Craig, L.C., Proc. Natl. Acad. Sci. 67:343, 1970.

46. Ramachandran, G.N., Ramakrishnan, C., and Sasisekharan, V., J. Mol. Biol. 7:95, 1963.

47. Karle, I.L., Biochemistry 13:2155, 1974.

48. Scheraga, H.A., IUPAC: Macromolecular MicroSymposia 10 and 11:1, 1972.

49. Johnson, C.E., Jr., and Bovey, F.A., J. Chem. Phys. 29:1012, 1958.

50. Bloembergen, N., Purcell, E.M., and Pound, R.V., Phys. Rev. 73:697, 1948.

51. Campbell, I.D., and Freeman, R., J. Magn. Resonance 11:143, 1973.

52. Coates, H.B., McLauchlan, K.A., Campbell, I.D., and McCall, C.E., Biochim. Biophys. Acta 310:1, 1973.

53. Breitmaier, E., Spohn, K.-H., and Berger, S., Angew. Chem., Internatl. Edit. 14:144, 1975.

54. McConnell, H.M., J. Chem. Phys. 28:430, 1958.

55. Molday, R.S., Englander, S.W., and Kallen, R.G., Biochemistry 11:150, 1972.

56. Emsley, J.W., Feeney, J., and Sutcliffe, L.H., "High Resolution Nuclear Magnetic Resonance Spectroscopy," pp. 20-25, Pergamon Press, Oxford, 1965.

57. Stern, A., Gibbons, W.A., and Craig, L.C., J. Amer. Chem. Soc. 91:2794, 1969.

58. Chen, R.F., Edelhoch, H., and Steiner, R.F., in "Physical Principles and Techniques of Protein Chemistry, Part A," Leach, S.J., Ed., p. 171, Academic Press, New York, 1969.

59. Laskowski, M., Jr., in "Spectroscopic Approaches to Biomolecular Conformation," Urry, D.W., Ed., p. 1, American Medical Association, Chicago, 1970.

60. Keil, B., Zikan, J., Rexova, L., and Sŏrm, F., Collection Czechoslov. Chem. Commun. 27:1678, 1962.

61. Stern, A., Doctoral Dissertation, The Rockefeller University, 1970.